AN ABSTRACT OF THE THESIS OF

Venkata Ramana Mallysetty for the degree of Master of Science in Mechanical Engineering presented on Feb 18, 1992.

Title: A Simplified Dynamic Model of the Hind Leg of a Beetle During Step Initiation

Abstract approved : Redacted for Privacy

Eugene F. Fichter

This thesis investigates a simple dynamic model of the hind leg of a beetle during initiation of a step. The primary assumption was that the full load of the body was carried on the hind leg during this time. That is, the only forces on the body were that of the hind leg and gravity and their resultant produced forward acceleration.

Only two dimensional models were used in this study. This was justified since the beetle is bilaterally symmetrical. However, it required the assumption that hind legs were positioned symmetrically and it limited the investigation to forward acceleration in a straight line.

Models with two and three links were tested. The two link

model assumed the body has no motion relative to the upper legs; that is the muscles were strong enough to prevent movement at the joint between body and leg. The three link model assumed only friction prevented movement at the joint between body and leg.

Dynamic equations were developed using Lagrangian mechanics. These equations were integrated using the 4th order Runge-Kutta algorithm. Both models were driven by applying a constant torque at the joint between upper and lower segments. Driving torque was adjusted to minimize verical movement of body center of mass.

Initial position of body center of mass relative to foot was varied to examine it's influence on both horizontal travel of body, center of mass and driving torque required for this travel.

For both models horizontal travel was less dependent on initial height of body center-of-mass than on initial horizontal position. For both models required driving torque increased with decrease in initial height of body center-of-mass and with increase of initial horizontal distance from foot to body center-of-mass. For both models maximum horizontal travel was attained with minimum initial height of body center-of-mass and minimum initial horizontal distance between foot and body center-of-mass. For the two link model, maximum horizontal travel was approximately half of the total leg length while for the three link model the equivalent number was approximately one quarter, of total leg length.

A Simplified Dynamic Model of the Hind Leg of a Beetle During Step Initiation

by
Venkata Ramana Mallysetty

A THESIS
submitted to
Oregon State University

in partial fulfillment of
the requirement for the
degree of

Master of Science

Completed by Feb 18, 1992
Commencement June, 1992

APPROVED:

Redacted for Privacy

Associate Professor of Mechanical Engineering
in charge of major

Redacted for Privacy

Head of Department of Mechanical Engineering

Redacted for Privacy

Dean of Graduate School

Date thesis is presented February 18, 1992

Presented by Venkata Ramana Mallysetty

Acknowledgements

Special thanks are due to Dr. Eugene F. Fichter, my major professor, and his wife Dr. Becky L. Fichter, for their invaluable advice and guidance, which made my thesis possible.

I would also like to thank all my teachers at Oregon State University for their advice and help. Thanks are also due to Dr. Gordon M. Reistad, Head of Mechanical Engineering Department, for his financial support for my graduate study. I would like to thank all the members of the "Walking Machines Group" for making research meetings fun and interesting.

I am deeply indebted to my parents and brothers for their love and affection. Finally, I would like to thank all my friends for their admirable patience and courage in coping up with my guitar music, and for not breaking the guitar into pieces and jumping on it's remains with hob nailed boots, as they originally threatened.

TABLE OF CONTENTS

LIST OF FIGURES

LIST OF TABLES

LIST OF APPENDIX FIGURES

A SIMPLIFIED DYNAMIC MODEL OF THE HIND LEG OF A BEETLE DURING STEP INITIATION

1. INTRODUCTION

1.1 Why walking machines?

The main purpose of walking machines is travel on uneven surfaces. If the surface were to be even, robots with wheels could work faster and more efficiently. Walking machines, or legged vehicles, have many advantages over wheeled machines. Walking machines are capable of travelling in difficult terrains, climbing steep inclines, traversing narrow beams and maneuvering around obstacles. These advantages make them useful in hazardous environments. Some of the many uses are in the maintenance of space stations and underwater structures.

In addition, they also have the advantages of having better fuel efficiency in rough terrain and, in comparison to wheeled or tracked vehicles, they cause less ground damage (Song & Waldron, 1989). Legs of walking machines may also be used as secondary arms for gripping or digging, or as counter weights to restore an overturned body to its feet (Todd, 1985).

The need for walking machines does not rule out the importance and advantages of wheeled robots. Each has advantages in different applications.

1.2 Why darkling beetle was chosen as a model?

Observing how easily, arthropods and vertebrates can walk on uneven surfaces, one realizes that they are excellent models for legged locomotion (Pedley, 1977; Gewecke & Wendler, 1985). The ability of these animals to avoid obstacles and adapt to a wide variety of surfaces has been a source of inspiration for walking machine research.

Vertebrates and arthropods have multi-segmented, articulated legs. Vertebrates have internal skeletons and sophisticated nervous system. Arthropods, including insects, spiders, crabs and lobsters, however, have external skeletons and simple nervous systems. Over the past 600 million years arthropods have evolved the ability to deal with a wide variety of terrains (Fichter et al., 1987).

For selecting an animal as a model for walking machine research one has to consider many aspects. For instance, the ease of analyzing the walking system of the model and type of task required. An animal with locomotion confined to walking or running would be an advantage.

It is desirable for a walking machine to possess good balance when at rest and when walking. Four legged and six legged machines can stand in one position and have good balance. However, six legs provide easier balance when walking. Alternating tripod gait, in which three legs are on the ground and the other three legs move forward, gives easier and better balance for walking.

The darkling beetle, Eleodes obscura sulcipennis, has been selected as a model for this research in walking machines because of its relatively simple leg mechanism and inability to fly or jump. These beetles are durable and easy to handle with body length about 30mm. Darkling beetles are commonly found in arid regions of the western USA.

1.3 Organization of the study

This report is divided into six parts. The first part, presented in Chapter 2, discusses the model development. The reason for considering the models and how the values of the model parameters are found are briefly described in this chapter. The selection of the various initial foot positions for the hind leg are also discussed along with a brief description of the characteristics analyzed.

Chapter 3, discusses approach used to develop and solve the equations of motion. The Lagrangian mechanics approach is used to obtain the equations of motion. Runge-Kutta fourth-order algorithm for numerical integration is used to integrate the equations of motion. Both the Lagrangian mechanics approach and the numerical integration method are briefly explained in this chapter.

The two link model of the hind leg is described in Chapter 4. The equations of motion are derived using the Lagrangian approach. The equations then, are converted to a convenient form for numerical

integration.

The three link model is described in Chapter 5. Equations of motion for this model are derived. A brief description of the static and dynamic friction torque, considered at joint 3 for this analysis, is given in this chapter. However, for ease of reading, the mathematical representation of the incorporation of the friction torque into the numerical integration procedure, is given in appendix A.4.

The discussion of the results for the two link model is presented in Chapter 6. The relationship between the initial foot position and the parameters is discussed in detail for this model.

The discussion of the results for the three link model is presented in Chapter 7. Foot positions other than the ones described in chapter 2, were considered in this chapter. The need for considering additional foot positions was explained. The relationships between initial position and the parameters are discussed in detail for this model.

Finally, in Chapter 8, the conclusions from the study are presented. The initial positions of the hind leg of the beetle, which results in better push off for initiating walking are discussed. Suggestions for future study are also presented in this chapter.

Derivations for determination of initial position for both two and three link models, rearranging the dynamic equations for three link model for numerical integration, incorporation of friction torque, are provided in appendix A. Flow charts for major modules of

the code are presented in appendix B. Except the graphics part, all the software is portable to any machine and any 'C' compiler, such as UNIX, TurboC.

2. BACKGROUND FOR THE DEVELOPMENT OF MODELS

2.1 Developing the model

Since this thesis only considers walking in a straight line and since the hind leg is nearly parallel to the body center line, only two dimensional models of the hind leg are considered for this thesis. Two dimensional models are simpler and thus, easier to evaluate than the three dimensional models and with the above simplifications they represent motion of the beetle quite well.

Two models, a two-link and a three-link model, are considered. These models are explained in more detail in chapters 4.1 and 5.1. Figure 2.1 gives the bottom view of the beetle, indicating the various joints of the hind leg.

The model parameters, that is, data for the lengths of the links, position of the center of mass and the masses of each of the links etc., were taken from Baek(1990) and from Fichter(unpublished). The lengths of the tibia and femur are 10.4mm and 11.9mm respectively. The total mass of the beetle is 1.1gm and the hind leg has a mass of 0.02gm. Thus, the tibia and femur have masses of 0.01gm each. The center of mass of the beetle is 2.2mm from the coxa-trochanter joint (Fichter, unpublished).

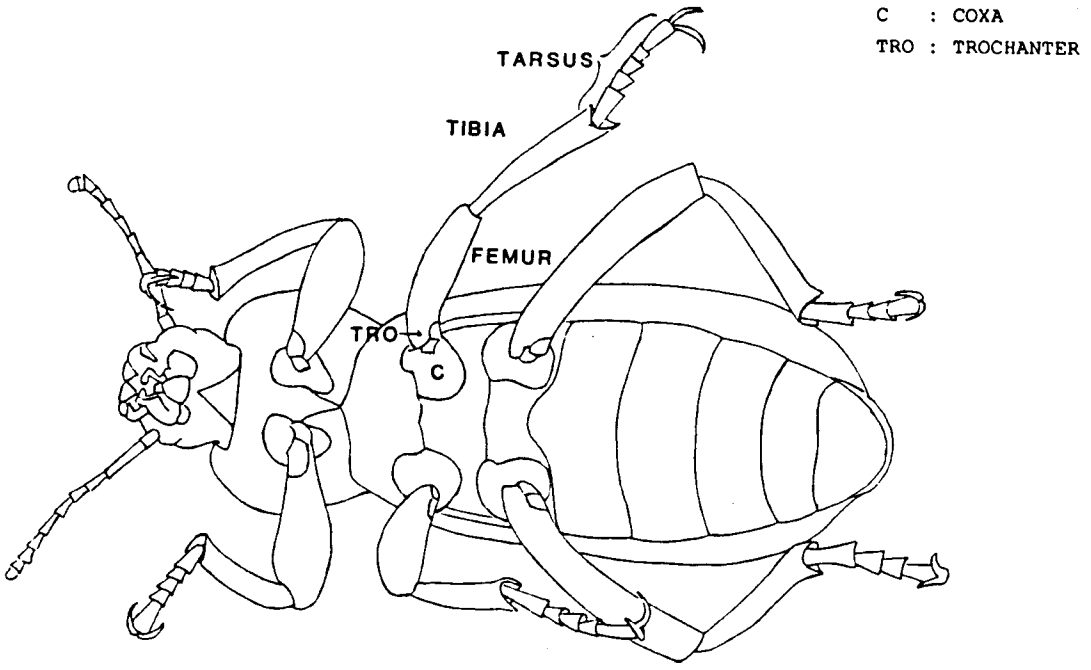

Fig 2.1 Beetle's bottom view

2.2 Initial positions

The normal resting height of the darkling beetle, determined from observation (Baek 1990), is with center of mass (cm) approximately 10mm above the ground (Ycm =

10mm). To get a better understanding of the effect of changes in body height upon the dynamic behavior, body heights 2mm above and below the normal resting height, that is, Ycm at 12mm and 8mm are also considered for analysis.

Selecting foot points at the middle of the maximum leg stroke provides the most freedom of body movement. At body height of 10mm, Baek(1990) found that the center of mass is 10mm in front of the hind foot when foot is at middle of maximum leg stroke. To evaluate change in horizontal distance between foot and CM two other positions of the foot were used; one 1/4 of maximum leg stroke in front and one 1/4 of maximum leg stroke behind the middle position. Thus, there are three possible x coordinates and three possible y coordinates of center of mass. From these, 9 initial positions are possible. All these coordinates are with respect to the foot. These initial positions of center of mass are indicated in Figure 2.2.

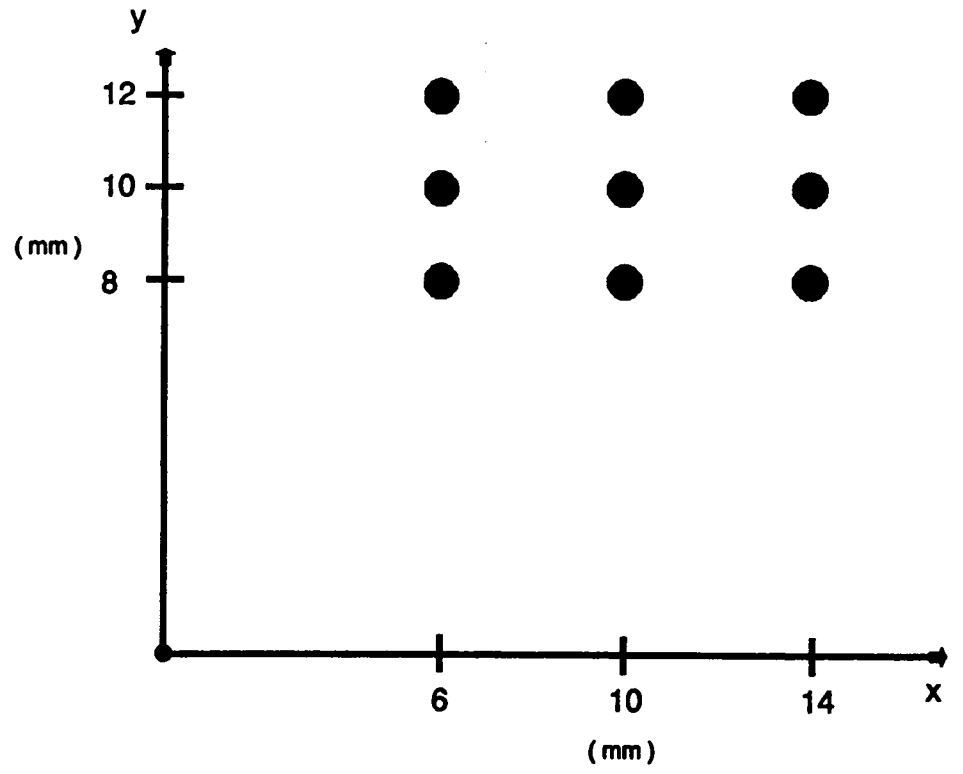

Fig 2.2 Initial positions of center of mass of the beetle

2.3 Characteristics to be studied

Several characteristics of the motion of the center of mass are to be determined, i) Trajectory ii) Time of travel iii) Travel in the X - direction (xtravel) and iv) Travel in the Y - direction (ytravel) of center of mass. Figure 2.3 illustrates the definitions for xtravel and ytravel for a two-link model.

Trajectory : Trajectory refers to the time history of position, velocity or acceleration of a particular point

of interest. In our case, we are interested in the trajectory of position of center of mass of the walking machine.

The trajectory of center of mass is an important factor in the study of dynamics of the walking machine. A smooth and flat trajectory uses less energy than other trajectories to do the same work. Only the push-off phase of walking is considered for analysis. That is, motion of hind leg of beetle from stationary position until there is a need to lift hind leg off the ground.

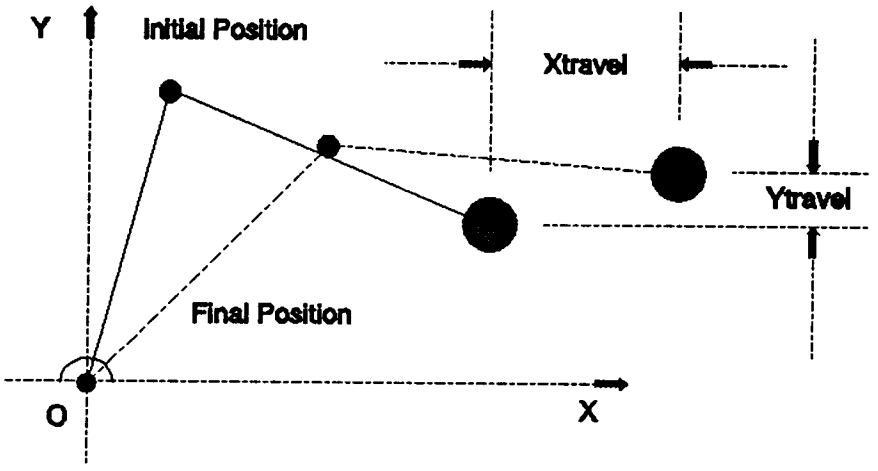

Fig 2.3 Definitions for xtravel and ytravel

Knowledge of dynamic behavior of walking machine for different foot positions can be used in maximizing forward travel, time of travel and linear velocity of center of mass of the walking machine.

Time of travel : It is the time taken for hind leg to reach the final position from the initial position.
xtravel : It is the amount of distance travelled in the x-direction before the limits on the leg are reached. This is shown in Figure 2.3.
ytravel : It is the amount of distance travelled in the y-direction before the limits on the leg are reached. This is the difference between value of the y-coordinate of the center of mass at the end of the run, from the initial value. This is shown in Figure 2.3.

3. APPROACH FOR DEVELOPING AND SOLVING DYNAMIC EQUATIONS

3.1 Lagrangian mechanics

Dynamic equations relate forces and torques to positions, velocities and accelerations. They are solved in order to obtain the equations of motion, that is, given forces and torques as input, these equations specify resulting motion of the system. A manipulator having 'n' degrees of freedom results in 'n' coupled, non-linear differential equations. By using dynamic simulation we will be able to predict the behavior of center of mass of the walking machine for any given initial position, and any given forces and torques. Lagrangian mechanics was used for this study.

The Lagrangian L is the difference between the kinetic energy K and the potential energy P of the system,

$$L = K - P \tag{3.1}$$

The kinetic and potential energy can be expressed in any convenient coordinate system that will simplify the problem. The dynamic equations, in terms of the coordinates used to express the kinetic and potential energy, are obtained as

$$F_i = \frac{d}{dt}\frac{\partial L}{\partial \dot{q}_i} - \frac{\partial L}{\partial q_i} \qquad (3.2)$$

Where q_i are the generalized coordinates in which the kinetic and potential energy are expressed, $\dot{q}_i$ is the generalized velocity, and F_i the force.

3.2 Runge-Kutta algorithm for numerical integration

As Equation 3.2 shows, dynamic equations involve differentials of the generalized co-ordinates. To obtain values of generalized coordinates, these dynamic equations were integrated using the fourth-order Runge-Kutta. At each step this method calculates the next step using the following equations

$k_1 = hf'(x_n, y_n)$

$k_2 = hf'(x_n+\frac{1}{2}h, y_n+\frac{1}{2}k_1)$

$k_3 = hf'(x_n+\frac{1}{2}h, y_n+\frac{1}{2}k_2)$

$k_4 = hf'(x_n+h, y_n+k_3)$

$$y_{n+1} = y_n+\frac{1}{6}(k_1+2k_2+2k_3+k_4)+O(h^5) \qquad (3.3)$$

where,

h is the step size, $O(h^5)$ represents terms of order 5 or greater, which are neglected,

$f(x_n, y_n)$ is a first-order differential equation and

$f'(x_n, y_n)$ is the derivative with respect to time.

For every iteration, k_1, k_2, k_3 and k_4 are evaluated and then the value of the function at the next step is obtained from Equation 3.3. The Runge-Kutta method treats every step in a sequence of steps identically. Prior behavior of a solution is not used in its propagation. This is mathematically proper, since any point along the trajectory of an ordinary differential equation can serve as an initial point. Further details are out of the scope of this thesis and interested reader can refer to Press etal (1988).

The fourth-order Runge-Kutta method requires four evaluations of the differential equations per step and is effective even with large step size for many problems. As this method is very stable and simple to use, this method was chosen for the numerical integration procedure for this thesis.

The formulas given are for integrating first order differential equations. However, the same formula can be used to solve second-order differential equations by converting the second order differential equations to first-order differential equations by defining new variables. Using this method, for every second-order differential equation, there are two first-order differential equations. These two first-order differential equations, then, can be solved using the method mentioned above.

4. TWO LINK MODEL

4.1 Two link model representation

The first model for the hind leg consists of two links. The first link is attached to ground at the foot and the second link connects first link to the body of the beetle. Both joints are revolute joints. The mass of the first link, 0.01gm, is considered to be a point mass at the end of the link. The mass of the beetle, 1.1gm, is concentrated at the end of the second link as shown in Figure 4.1.

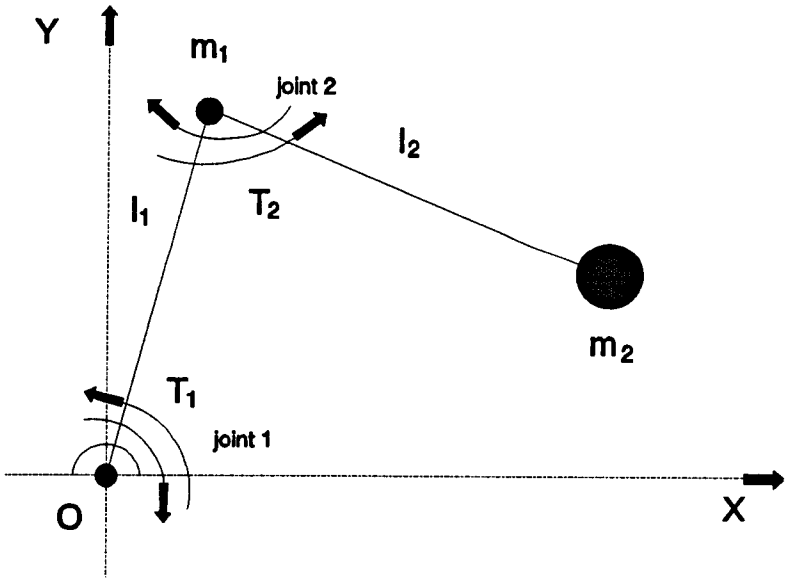

Fig 4.1 Two link model representation

There are no forces on the system except gravity. Since, beetle does not have muscles big enough to exert any torque at the foot the only driving torque is applied at joint 2.

Figure 4.2, illustrates the co-ordinate system and the generalized co-ordinates for the model. x_c and y_c are co-ordinates of the center of mass. The values of θ_1 and θ_2 can be obtained for given x and y co-ordinates of the initial position of center of mass. The derivation is given in appendix A.1.

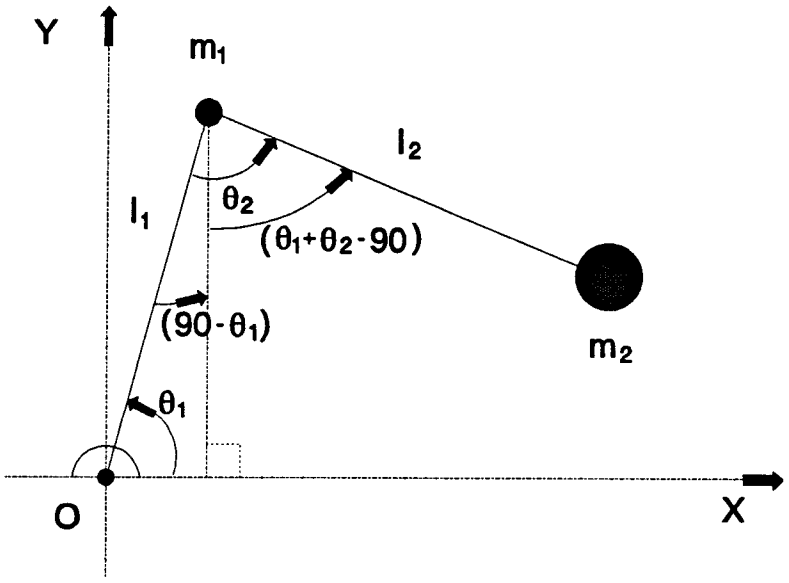

Fig 4.2 Representation of generalized co-ordinates for the two link model

Co-ordinates of joint 2 are (x_1, y_1) and co-ordinates of center of mass are (x_c, y_c), also represented by (x_2, y_2).

4.2 Developing equations of motion for the 2-link model

Link 1 : Kinetic energy and potential energy of the first link are given by,

$$K_1 = \tfrac{1}{2} m_1 l_1^2 \dot{\theta}_1^2 \tag{4.1}$$

$$P_1 = m_1 g l_1 \sin\theta_1 \tag{4.2}$$

Link 2 :

$$x_2 = l_1\cos\theta_1 - l_2\cos(\theta_1+\theta_2)$$

$$y_2 = l_1\sin\theta_1 - l_2\sin(\theta_1+\theta_2)$$

$$\dot{x}_2 = - l_1\dot{\theta}_1\sin\theta_1 + l_2(\dot{\theta}_1+\dot{\theta}_2)\sin(\theta_1+\theta_2)$$

$$\dot{y}_2 = l_1\dot{\theta}_1\cos\theta_1 - l_2(\dot{\theta}_1+\dot{\theta}_2)\cos(\theta_1+\theta_2)$$

$$v_2^2 = \dot{x}_2^2 + \dot{y}_2^2$$

$$\therefore v_2^2 = l_1^2\dot{\theta}_1^2 + l_2^2 (\dot{\theta}_1+\dot{\theta}_2)^2 - 2l_1l_2\dot{\theta}_1(\dot{\theta}_1+\dot{\theta}_2)\cos\theta_2$$

Thus, kinetic and potential energy of the second link are given by,

$$K_2 = \tfrac{1}{2} m_2 v_2^2$$

$$\therefore K_2 = \tfrac{1}{2}m_2l_1^2\dot{\theta}_1^2+\tfrac{1}{2}m_2l_2^2 (\dot{\theta}_1+\dot{\theta}_2)^2-m_2l_1l_2\dot{\theta}_1(\dot{\theta}_1+\dot{\theta}_2)\cos\theta_2 \tag{4.3}$$

$$P_2 = m_2 g y_2$$

$$\therefore P_2 = m_2 g(l_1\sin\theta_1-l_2\sin(\theta_1+\theta_2)) \tag{4.4}$$

and the Lagrangian is given by, according to Equation 3.1

$$L = K - P = (K_1+K_2) - (P_1+P_2)$$

$$\therefore L = \tfrac{1}{2}(m_1+m_2)l_1^2\dot{\theta}_1^2+\tfrac{1}{2}m_2l_2^2(\dot{\theta}_1+\dot{\theta}_2)^2-m_2l_1l_2\dot{\theta}_1(\dot{\theta}_1+\dot{\theta}_2)\cos\theta_2$$

$$- (m_1+m_2)gl_1\sin\theta_1+m_2gl_2\sin(\theta_1+\theta_2)) \tag{4.5}$$

Torque at joint 1:

$$\frac{\partial L}{\partial \dot{\theta}_1} = (m_1+m_2)l_1^2\dot{\theta}_1+m_2l_2^2(\dot{\theta}_1+\dot{\theta}_2)-m_2l_1l_2\dot{\theta}_1(2\dot{\theta}_1+\dot{\theta}_2)\cos\theta_2 \tag{4.6}$$

$$\frac{d}{dt}\frac{\partial L}{\partial \dot{\theta}_1} = ((m_1+m_2)l_1^2+m_2l_2^2-2m_2l_1l_2\cos\theta_2)\ddot{\theta}_1+(m_2l_2^2-$$

$$2m_2l_1l_2\cos\theta_2)\ddot{\theta}_2+2m_2l_1l_2\dot{\theta}_1\dot{\theta}_2\sin\theta_2+m_2l_1l_2\dot{\theta}_2^2\sin\theta_2 \tag{4.7}$$

$$\frac{\partial L}{\partial \theta_1} = -(m_1+m_2)gl_1\cos\theta_1+m_2gl_2\cos(\theta_1+\theta_2) \tag{4.8}$$

Combining Equations 4.6, 4.7 and 4.8 according to 3.2 gives

$$T_1 = D_{11}\ddot{\theta}_1 + D_{12}\ddot{\theta}_2 + D_{122}\dot{\theta}_2^2 + D_{112}\dot{\theta}_1\dot{\theta}_2 + D_1 \tag{4.9}$$

where,

$D_{11} = (m_1+m_2)l_1^2+m_2l_2^2-2m_2l_1l_2\cos\theta_2$

$D_{12} = m_2l_2^2-m_2l_1l_2\cos\theta_2$

$D_{122} = m_2l_1l_2\sin\theta_2$

$D_{112} = 2m_2l_1l_2\sin\theta_2$

$D_1 = (m_1+m_2)gl_1\cos\theta_1 - m_2gl_2\cos(\theta_1+\theta_2)$

Torque at joint 2:

$$\frac{\partial L}{\partial \dot{\theta}_2} = m_2l_2^2\dot{\theta}_1+m_2l_2^2\dot{\theta}_2-m_2l_1l_2\dot{\theta}_1\cos\theta_2 \tag{4.10}$$

$$\frac{d}{dt}\frac{\partial L}{\partial \dot{\theta}_2} = (m_2l_2^2-m_2l_1l_2\cos\theta_2)\ddot{\theta}_1+m_2l_2^2\ddot{\theta}_2+m_2l_1l_2\dot{\theta}_1\dot{\theta}_2\sin\theta_2 \tag{4.11}$$

$$\frac{\partial L}{\partial \theta_2} = m_2l_1l_2\dot{\theta}_1(\dot{\theta}_1+\dot{\theta}_2)\sin\theta_2+m_2gl_2\cos(\theta_1+\theta_2) \tag{4.12}$$

Thus, combining equations 4.10, 4.11 and 4.12 according to 3.2, T_2 is given by,

$$T_2 = D_{12}\ddot{\theta}_1 + D_{22}\ddot{\theta}_2 + D_{211}\dot{\theta}_1^2 + D_2 \tag{4.13}$$

where,

$D_{22} = m_2l_2^2$

$D_{211} = - m_2l_1l_2\sin\theta_2$

$D_2 = - m_2 g l_2 \cos(\theta_1+\theta_2))$

Expressions for T_1 and T_2 are the dynamic equations to be used for simulation. Therefore, these are solved for $\ddot{\theta}_1$ and $\ddot{\theta}_2$. Information about the generalized co-ordinates and speeds can be obtained by integrating the expressions for $\ddot{\theta}_1$ and $\ddot{\theta}_2$. Equations 4.9 and 4.13 can be rearranged with only the accelerations on the left hand side as,

$D_{11}\ddot{\theta}_1 + D_{12}\ddot{\theta}_2 = T_1 - D_{122}\dot{\theta}_2^2 - D_{112}\dot{\theta}_1\dot{\theta}_2 - D_1$

$D_{12}\ddot{\theta}_1 + D_{22}\ddot{\theta}_2 = T_2 - D_{211}\dot{\theta}_1^2 - D_2$

Solving the above simultaneous equations for $\ddot{\theta}_1$ and $\ddot{\theta}_2$,

$\ddot{\theta}_1 = C_1+C_2\dot{\theta}_1^2+C_3\dot{\theta}_2^2+C_4\dot{\theta}_1\dot{\theta}_2+C_5$

$\ddot{\theta}_2 = E_1+E_2\dot{\theta}_1^2+E_3\dot{\theta}_2^2+E_4\dot{\theta}_1\dot{\theta}_2+E_5$

where,

$C = D_{11}D_{22}-D_{12}^2$

$C_1 = (T_1D_{22}-T_2D_{12})/C$

$C_2 = D_{12}D_{211}/C$

$C_3 = - D_{22}D_{122}/C$

$C_4 = - D_{22}D_{112}/C$

$C_5 = (D_2D_{12}-D_1D_{22})/C$

and,

$E = D_{12}^2-D_{11}D_{22}$

$E_1 = (T_1D_{12}-T_2D_{11})/E$

$E_2 = D_{11}D_{211})/E$

$E_3 = - D_{12}D_{122}/E$

$E_4 = - D_{12}D_{112}/E$

$E_5 = (D_2D_{11}-D_1D_{12})/E$

5. THREE LINK MODEL

5.1 Model representation

This model for the hind leg is similar to the model described in chapter 4, except that center of mass is not at the end of the second link. The third link represents the beetle body with concentrated mass. Also, masses of the first and second links are concentrated at the center

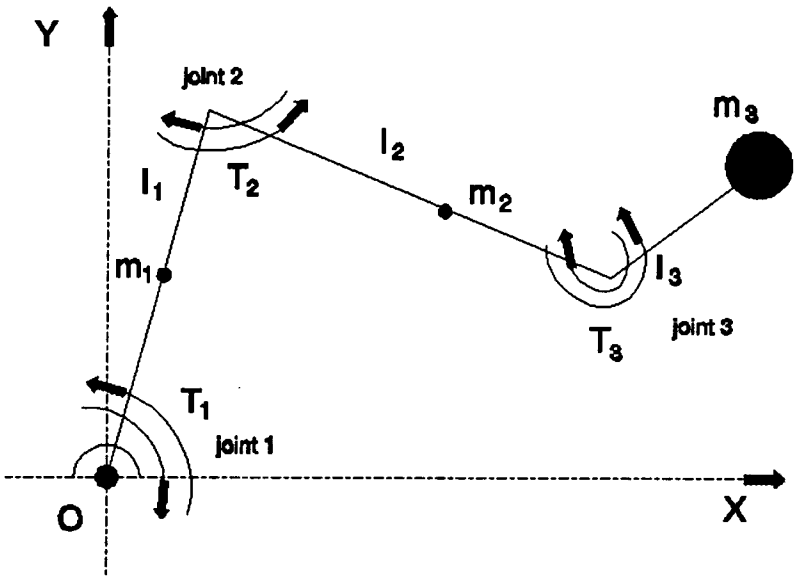

Fig 5.1 Three link model representation

of the respective links. No torque is applied at joint 3. However, static and dynamic friction effects are considered at this joint. The model is shown in Figure 5.1.

Friction torque and it's effects

From the initial runs with no torque at joint 3, I found that there is no stable position for the system, and the system collapses very fast. This led me to believe that there must be some kind of system of muscles acting at this joint. We have no information about this at this time. Thus, friction torque at joint 3 is an effort to model these unknown forces and torques. An exact number for this friction torque is very difficult to determine and not available at this time. From my initial runs, at least a value of 10 gm-cm^2/sec^2 for friction torque resulted in good xtravel and time of travel. Thus, this value is used for our analysis.

As long as the torque on joint 3 is less than the friction torque, there is no movement at the third joint. Thus, the velocity and acceleration of angle θ_3 is zero. However, once this static friction is overcome, the dynamic friction is valid and this friction torque acts in a direction opposing the motion of the third link. This can be mathematical represented as

$$\text{if} \quad |t_3| \leq t_f \qquad \ddot{\theta} = 0$$

$$\text{else} \quad T_3 = \left(|t_3| - t_f \right) \frac{t_3}{|t_3|}$$

Here, t_3 is the torque required at joint 3 for zero θ_3 acceleration, t_f is the friction torque at joint 3, and T_3 is the torque causing acceleration at joint 3. The incorporation of the friction torque into the software is explained in Appendix A.4.

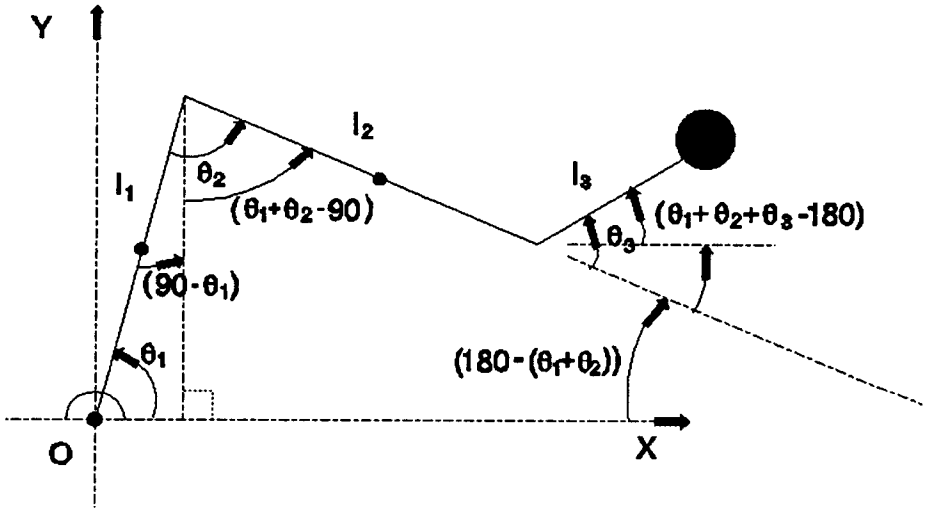

Fig 5.2 Representation of generalized co-ordinates for the three link model

Figure 5.2, illustrates the co-ordinate system, and generalized co-ordinates for the model. x_c and y_c are co-ordinates of the center of mass. The values of θ_1 , θ_2, and θ_3 can be obtained for given x and y co-ordinates of the initial position of the center of mass. The derivation is given in appendix A.2.

5.2 Equations of motion for the 3-link model

The position of the center of mass can be described by

$$x_c = l_1\cos\theta_1 - l_2\cos(\theta_1+\theta_2) - l_3\cos(\theta_1+\theta_2+\theta_3) \quad (5.1)$$

$$y_c = l_1\sin\theta_1 - l_2\sin(\theta_1+\theta_2) - l_3\sin(\theta_1+\theta_2+\theta_3) \quad (5.2)$$

Differentiating equations 5.1 and 5.2 results in

$$\dot{x}_c = - l_1\dot{\theta}_1\sin\theta_1 + l_2(\dot{\theta}_1+\dot{\theta}_2)\sin(\theta_1+\theta_2) + l_3(\dot{\theta}_1+\dot{\theta}_2+\dot{\theta}_3)\sin(\theta_1+\theta_2+\theta_3)$$

$$\dot{y}_c = l_1\dot{\theta}_1\cos\theta_1 - l_2(\dot{\theta}_1+\dot{\theta}_2)\cos(\theta_1+\theta_2) + l_3(\dot{\theta}_1+\dot{\theta}_2+\dot{\theta}_3)\cos(\theta_1+\theta_2+\theta_3)$$

Kinetic and Potential energy :-

Link 1

The kinetic and potential energies of first link are given by,

$$K_1 = \tfrac{1}{2}\, m_1 l_1^2 \dot{\theta}_1^2 \quad (5.3)$$

$$P_1 = m_1 g l_1 \sin\theta_1 \quad (5.4)$$

Link 2 :

As the mass is concentrated at the center of the link,

$x_2 = l_1\cos\theta_1 - \frac{1}{2}l_2\cos(\theta_1+\theta_2)$

$y_2 = l_1\sin\theta_1 - \frac{1}{2}l_2\sin(\theta_1+\theta_2)$

differentiating once results in,

$\dot{x}_2 = -l_1\dot{\theta}_1\sin\theta_1 + \frac{1}{2}l_2(\dot{\theta}_1+\dot{\theta}_2)\sin(\theta_1+\theta_2)$

$\dot{x}_2 = l_1\dot{\theta}_1\cos\theta_1 - \frac{1}{2}l_2(\dot{\theta}_1+\dot{\theta}_2)\cos(\theta_1+\theta_2)$

$v_2^2 = \dot{x}_2^2 + \dot{y}_2^2$

$\therefore v_2^2 = l_1^2\dot{\theta}_1^2 + \frac{1}{4}l_2^2(\dot{\theta}_1+\dot{\theta}_2)^2 - l_1l_2\dot{\theta}_1(\dot{\theta}_1+\dot{\theta}_2)\cos\theta_2$

Thus, kinetic and potential energies are given by,

$$K_2 = \frac{1}{2}m_2l_1^2\dot{\theta}_1^2+\frac{1}{8}m_2l_2^2(\dot{\theta}_1+\dot{\theta}_2)^2-\frac{1}{2}m_2l_1l_2\dot{\theta}_1(\dot{\theta}_1+\dot{\theta}_2)\cos\theta_2 \qquad (5.5)$$

$$P_2 = m_2g(l_1\sin\theta_1-\frac{1}{2}l_2\sin(\theta_1+\theta_2)) \qquad (5.6)$$

Link 3

$v_3^2 = \dot{x}_c^2 + \dot{y}_c^2$

substituting the expressions for velocities of x_c and y_c and simplifying the terms, results in

$$v_3^2 = l_1^2\dot{\theta}_1^2+l_2^2(\dot{\theta}_1+\dot{\theta}_2)^2+l_3^2(\dot{\theta}_1+\dot{\theta}_2+\dot{\theta}_3)^2-2l_1l_2\dot{\theta}_1(\dot{\theta}_1+\dot{\theta}_2)\cos\theta_2$$
$$+ 2l_2l_3(\dot{\theta}_1+\dot{\theta}_2)(\dot{\theta}_1+\dot{\theta}_2+\dot{\theta}_3)\cos\theta_3-2l_1l_3\dot{\theta}_1(\dot{\theta}_1+\dot{\theta}_2+\dot{\theta}_3)\cos(\theta_2+\theta_3)$$

the kinetic and potential energy are given by,

$$K_3 = \frac{1}{2}m_3l_1^2\dot{\theta}_1^2+\frac{1}{2}m_3l_2^2(\dot{\theta}_1+\dot{\theta}_2)^2+\frac{1}{2}m_3l_3^2(\dot{\theta}_1+\dot{\theta}_2+\dot{\theta}_3)^2- m_3l_1l_2\dot{\theta}_1$$
$$(\dot{\theta}_1+\dot{\theta}_2)\cos\theta_2+m_3l_2l_3(\dot{\theta}_1+\dot{\theta}_2)(\dot{\theta}_1+\dot{\theta}_2+\dot{\theta}_3)\cos\theta_3$$
$$-m_3l_1l_3\dot{\theta}_1(\dot{\theta}_1+\dot{\theta}_2+\dot{\theta}_3)\cos(\theta_2+\theta_3) \qquad (5.7)$$

$$P_3 = m_3g(l_1\sin\theta_1-l_2\sin(\theta_1+\theta_2)-l_3\sin(\theta_1+\theta_2+\theta_3)) \qquad (5.8)$$

According to Equation 3.1, the Lagrangian would be

$L = K - P = (K_1+K_2+K_3) - (P_1+P_2+P_3)$

Combining Equations 5.3 through 5.8 and simplifying would result in

$$L = \tfrac{1}{2}(m_1+m_2+m_3)\,l_1^2\dot{\theta}_1^2+\tfrac{1}{2}(\tfrac{1}{4}m_2+m_3)\,l_2^2\,(\dot{\theta}_1+\dot{\theta}_2)^2+\tfrac{1}{2}m_3l_3^2$$
$$(\dot{\theta}_1+\dot{\theta}_2+\dot{\theta}_3)^2-(\tfrac{1}{2}m_2+m_3)\,l_1l_2\dot{\theta}_1(\dot{\theta}_1+\dot{\theta}_2)\cos\theta_2+m_3l_2l_3(\dot{\theta}_1+\dot{\theta}_2)$$
$$(\dot{\theta}_1+\dot{\theta}_2+\dot{\theta}_3)\cos\theta_3-m_3l_1l_3\dot{\theta}_1(\dot{\theta}_1+\dot{\theta}_2+\dot{\theta}_3)\cos(\theta_2+\theta_3)$$
$$-(\tfrac{1}{2}m_1+m_2+m_3)\,gl_1\sin\theta_1+(m_2+m_3)\,gl_2\sin(\theta_1+\theta_2)+$$
$$m_3gl_3\sin(\theta_1+\theta_2+\theta_3) \qquad (5.9)$$

The general expression for torque is given by,

$$T_i = \frac{d}{dt}\frac{\partial L}{\partial \dot{\theta}_i} - \frac{\partial L}{\partial \theta_1} \qquad \text{for } i = 1,\ 2,\ 3 \qquad (5.10)$$

Torque at joint 1 :

$$\frac{\partial L}{\partial \dot{\theta}_1} = (m_1+m_2+m_3)\,l_1^2\dot{\theta}_1+(\tfrac{1}{4}m_2+m_3)\,l_2^2(\dot{\theta}_1+\dot{\theta}_2)+m_3l_3^2(\dot{\theta}_1+\dot{\theta}_2+\dot{\theta}_3)$$
$$-(\tfrac{1}{2}m_2+m_3)\,l_1l_2(2\dot{\theta}_1+\dot{\theta}_2)\cos\theta_2+m_3l_2l_3(2\dot{\theta}_1+2\dot{\theta}_2+\dot{\theta}_3)\cos\theta_3$$
$$-m_3l_1l_3(2\dot{\theta}_1+\dot{\theta}_2+\dot{\theta}_3)\cos(\theta_2+\theta_3)$$

$$\frac{d}{dt}\frac{\partial L}{\partial \dot{\theta}_1} = (m_1+m_2+m_3)\,l_1^2\ddot{\theta}_1+(\tfrac{1}{4}m_2+m_3)\,l_2^2(\ddot{\theta}_1+\ddot{\theta}_2)+m_3l_3^2(\dot{\theta}_1+\dot{\theta}_2+\dot{\theta}_3)$$
$$-(\tfrac{1}{2}m_2+m_3)\,l_1l_2(\ddot{\theta}_1+\ddot{\theta}_2)\cos\theta_2+(\tfrac{1}{2}m_2+m_3)\,l_1l_2\dot{\theta}_2(2\dot{\theta}_1+\dot{\theta}_2)\sin\theta_2$$
$$+m_3l_2l_3(2\ddot{\theta}_1+2\ddot{\theta}_2+\ddot{\theta}_3)\cos\theta_3-m_3l_2l_3\dot{\theta}_3(2\dot{\theta}_1+2\dot{\theta}_2+\dot{\theta}_3)\sin\theta_3$$
$$-m_3l_1l_3(2\ddot{\theta}_1+\ddot{\theta}_2+\ddot{\theta}_3)\cos(\theta_2+\theta_3)+m_3l_1l_3(\dot{\theta}_2+\dot{\theta}_3)$$
$$(2\dot{\theta}_1+\dot{\theta}_2+\dot{\theta}_3)\sin(\theta_2+\theta_3)$$

$$\frac{\partial L}{\partial \theta_1} = -(\tfrac{1}{2}m_1+m_2+m_3)\,gl_1\cos\theta_1+(\tfrac{1}{2}m_2+m_3)\,gl_2\cos(\theta_1+\theta_2)$$
$$+\ m_3gl_3\cos(\theta_1+\theta_2+\theta_3)$$

Adding the terms according to Equation 3.2,

$$T_1 = a_1\ddot{\theta}_1+a_2\ddot{\theta}_2+a_3\ddot{\theta}_3+a_4\dot{\theta}_1^2+a_5\dot{\theta}_2^2+a_6\dot{\theta}_3^2+a_7\dot{\theta}_1\dot{\theta}_2+a_8\dot{\theta}_2\dot{\theta}_3+a_9\dot{\theta}_3\dot{\theta}_1+a_{10} \qquad (5.11)$$

where,

$$a_1 = (m_1+m_2+m_3)\,l_1^2+(\tfrac{1}{4}m_2+m_3)\,l_2^2+m_3l_3^2-2(\tfrac{1}{2}m_2+m_3)\,l_1l_2\cos\theta_2$$
$$+2m_3l_2l_3\cos\theta_3-2m_3l_1l_3\cos(\theta_2+\theta_3)$$

$$a_2 = (\tfrac{1}{4}m_2+m_3)\,l_2^2+m_3l_3^2-(\tfrac{1}{2}m_2+m_3)\,l_1l_2\cos\theta_2+2m_3l_2l_3\cos\theta_3 - m_3l_1l_3\cos(\theta_2+\theta_3)$$

$$a_3 = m_3l_3^2+m_3l_2l_3\cos\theta_3-m_3l_1l_3\cos(\theta_2+\theta_3)$$

$$a_4 = 0$$

$$a_5 = (\tfrac{1}{2}m_2+m_3)\,l_1l_2\sin\theta_2+m_3l_1l_3\sin(\theta_2+\theta_3)$$

$$a_6 = m_3l_1l_3\sin(\theta_2+\theta_3)-m_3l_2l_3\sin\theta_3$$

$$a_7 = 2(\tfrac{1}{2}m_2+m_3)\,l_1l_2\sin\theta_2+2m_3l_1l_3\sin(\theta_2+\theta_3)$$

$$a_8 = 2m_3l_1l_3\sin(\theta_2+\theta_3)-2m_3l_2l_3\sin\theta_3$$

$$a_9 = 2m_3l_1l_3\sin(\theta_2+\theta_3)-2m_3l_2l_3\sin\theta_3$$

$$a_{10} = (\tfrac{1}{2}m_1+m_2+m_3)\,gl_1\cos\theta_1-(\tfrac{1}{2}m_2+m_3)\,gl_2\cos(\theta_1+\theta_2) - m_3gl_3\cos(\theta_1+\theta_2+\theta_3)$$

Torque at joint 2 :

$$\frac{\partial L}{\partial \dot{\theta}_2} = (\tfrac{1}{4}m_2+m_3)\,l_2^2(\dot{\theta}_1+\dot{\theta}_2)+m_3l_3^2(\dot{\theta}_1+\dot{\theta}_2+\dot{\theta}_3)-(\tfrac{1}{2}m_2+m_3)\,l_1l_2\dot{\theta}_1\cos\theta_2 + m_3l_2l_3(2\dot{\theta}_1+2\dot{\theta}_2+\dot{\theta}_3)\cos\theta_3-m_3l_1l_3\dot{\theta}_1\cos(\theta_2+\theta_3)$$

$$\frac{d}{dt}\frac{\partial L}{\partial \dot{\theta}_2} = (\tfrac{1}{4}m_2+m_3)\,l_2^2(\ddot{\theta}_1+\ddot{\theta}_2)+m_3l_3^2(\ddot{\theta}_1+\ddot{\theta}_2+\ddot{\theta}_3)-(\tfrac{1}{2}m_2+m_3)\,l_1l_2\ddot{\theta}_1\cos\theta_2 + (\tfrac{1}{2}m_2+m_3)\,l_1l_2\dot{\theta}_1\dot{\theta}_2\sin\theta_2+m_3l_2l_3(2\ddot{\theta}_1+2\ddot{\theta}_2+\ddot{\theta}_3)-m_3l_2l_3\dot{\theta}_3(2\dot{\theta}_1+2\dot{\theta}_2+\dot{\theta}_3)\sin\theta_3 - m_3l_1l_3\ddot{\theta}_1\cos(\theta_2+\theta_3)+m_3l_1l_3\dot{\theta}_1(\dot{\theta}_2+\dot{\theta}_3)$$

$$\frac{\partial L}{\partial \theta_2} = (\tfrac{1}{2}m_2+m_3)\,l_1l_2\dot{\theta}_1(\dot{\theta}_1+\dot{\theta}_2)\sin\theta_2+m_3l_1l_3\dot{\theta}_1(\dot{\theta}_1+\dot{\theta}_2+\dot{\theta}_3)\sin(\theta_2+\theta_3) + (\tfrac{1}{2}m_2+m_3)\,gl_2\cos(\theta_1+\theta_2)+m_3gl_3\cos(\theta_1+\theta_2+\theta_3)$$

Combining the above three equations according to Equation 3.2 and simplifying would result in an expression for T_2 as

$$T_2 = b_1\ddot{\theta}_1+b_2\ddot{\theta}_2+b_3\ddot{\theta}_3+b_4\dot{\theta}_1^2+b_5\dot{\theta}_2^2+b_6\dot{\theta}_3^2+b_7\dot{\theta}_1\dot{\theta}_2+b_8\dot{\theta}_2\dot{\theta}_3+b_9\dot{\theta}_3\dot{\theta}_1+b_{10} \quad (5.12)$$

where,

$$b_1 = (\tfrac{1}{4}m_2+m_3)\,l_2^2+m_3l_3^2-(\tfrac{1}{2}m_2+m_3)\,l_1l_2\cos\theta_2 +2m_3l_2l_3\cos\theta_3-m_3l_1l_3\cos(\theta_2+\theta_3)$$

$$b_2 = (\tfrac{1}{4}m_2+m_3)\,l_2^2+m_3l_3^2+2m_3l_2l_3\cos\theta_3$$

$$b_3 = m_3l_3^2+m_3l_2l_3\cos\theta_3$$

$$b_4 = -(\tfrac{1}{2}m_2+m_3)\,l_1l_2\sin\theta_2-m_3l_1l_3\sin(\theta_2+\theta_3)$$

$$b_5 = 0$$

$$b_6 = -m_3l_2l_3\sin\theta_3$$

$$b_7 = 0$$

$$b_8 = -2m_3l_2l_3\sin\theta_3$$

$$b_9 = -2m_3l_2l_3\sin\theta_3$$

$$b_{10} = -(\tfrac{1}{2}m_2+m_3)\,gl_2\cos(\theta_1+\theta_2)-m_3gl_3\cos(\theta_1+\theta_2+\theta_3)$$

For Torque at joint 3 :

$$\frac{\partial L}{\partial \dot{\theta}_3} = m_3l_3^2(\dot{\theta}_1+\dot{\theta}_2+\dot{\theta}_3)+m_3l_2l_3(\dot{\theta}_1+\dot{\theta}_2)\cos\theta_3-m_3l_1l_3\dot{\theta}_1\cos(\theta_2+\theta_3)$$

$$\frac{d}{dt}\frac{\partial L}{\partial \dot{\theta}_3} = m_3l_3^2(\ddot{\theta}_1+\ddot{\theta}_2+\ddot{\theta}_3)-m_3l_2l_3(\ddot{\theta}_1+\ddot{\theta}_2)\cos\theta_3-m_3l_2l_3\dot{\theta}_3(\dot{\theta}_1+\dot{\theta}_2)\sin\theta_3 -m_3l_1l_3\ddot{\theta}_1\cos(\theta_2+\theta_3)+m_3l_1l_3\dot{\theta}_1(\dot{\theta}_2+\dot{\theta}_3)\sin(\theta_2+\theta_3)$$

$$\frac{\partial L}{\partial \theta_3} = -m_3l_2l_3(\dot{\theta}_1+\dot{\theta}_2)(\dot{\theta}_1+\dot{\theta}_2+\dot{\theta}_3)\sin\theta_3+m_3l_1l_3\dot{\theta}_1(\dot{\theta}_1+\dot{\theta}_2+\dot{\theta}_3)\sin(\theta_2+\theta_3) +m_3gl_3\cos(\theta_1+\theta_2+\theta_3)$$

Combining the above three equations according to Equation 3.2 and simplifying the terms results in an expression for T_3 as

$$T_3 = c_1\ddot{\theta}_1+c_2\ddot{\theta}_2+c_3\ddot{\theta}_3+c_4\dot{\theta}_1^2+c_5\dot{\theta}_2^2+c_6\dot{\theta}_3^2+c_7\dot{\theta}_1\dot{\theta}_2+c_8\dot{\theta}_2\dot{\theta}_3+c_9\dot{\theta}_3\dot{\theta}_1+c_{10} \quad (5.13)$$

where,

$c_1 = m_3l_3^2+m_3l_2l_3\cos\theta_3-m_3l_1l_3\cos(\theta_2+\theta_3)$

$c_2 = m_3l_3^2+m_3l_2l_3\cos\theta_3$

$c_3 = m_3l_3^2$

$c_4 = -m_3l_1l_3\sin(\theta_2+\theta_3)+m_3l_2l_3\sin\theta_3$

$c_5 = m_3l_2l_3\sin\theta_3$

$c_6 = 0$

$c_7 = 2m_3l_2l_3\sin\theta_3$

$c_8 = c_9 = 0$

$c_{10} = -m_3gl_3\cos(\theta_1+\theta_2+\theta_3)$

The dynamic equations are the expressions for torques at joints 1, 2 and 3, given by Equations 5.11, 5.12, and 5.13, to be used for simulation. These are solved for $\ddot{\theta}_1$, $\ddot{\theta}_2$ and $\ddot{\theta}_3$ to arrange in convenient form for numerical integration. This derivation and the incorporation of friction torque into the integration procedure are given in Appendix A.3 and A.4 respectively.

6. ANALYSIS FOR THE TWO LINK MODEL

This chapter discusses the results for the two link model. As mentioned in chapter 2.3 the parameters analyzed are i) Trajectory ii) Time of travel iii) Travel in the x - direction of center of mass (xtravel) and iv) Travel in the y - direction of center of mass (ytravel). Though the program calculates the linear velocity of the center of mass, it was not considered in the present analysis. However, at a later stage, it would be an important factor to be considered, and thus, it is provided in the software.

Constraints

Not all the information we get from integrating the equations of motion is useful. Thus, some constraints are imposed to cut down the unnecessary data. These constraints are

1. θ_1 : $0° <= \theta_1 >= 180°$
2. θ_2 : $40° <= \theta_2 >= 140°$
3. Height of center of mass: The height of center of mass must always be greater than zero, that is, above ground level.

From Figure 4.2, we can see that, if θ_1 is less than or equal to 0°, the first link is on the ground. This is

same for θ_1 of 180° or more. This is not desirable and thus, constraint 1 is imposed. The same constraint can be imposed on θ_2 for similar reasons. But, values of θ_2 very close to 0° or 180° are not very useful for our analysis. Because, this would mean that links one and two are either doubled up or in the same line. Thus, constraint 2 is imposed. The limits of 40° and 140° on θ_2 are chosen arbitrarily.

In the program, as soon as any of the above constraints are violated, the numerical integration is stopped and the data is stored in output files.

Results of the output runs:

For each initial position, the value of T_2 is varied until the required trajectory is obtained, i.e., flat trajectory with ytravel of 0 ± 0.2mm. For each initial position, T_2, time of travel, xtravel, and ytravel are tabulated.

Table 6.1 gives the results of all the runs for this model. From this data, plots can be made between various parameters. This will help understand the effect of one parameter over other parameters. T_2, the input variable, is the parameter being controlled. Thus, it will be useful to understand the effect of T_2 over other parameters, i.e., time of travel, xtravel and ytravel.

This gives us an understanding of the dynamic behavior of the leg.

Initial Pos. set no.	x_m (mm)	y_m (mm)	T_2 (gm-cm²/ sec²)	Time of travel (mSec)	xtravel (mm)	ytravel (mm)
1	6	8	1300 1400 1450 1500	56.7 53.9 52.6 51.3	13.1 12.4 12.3 12.2	-1.5 -0.2 0.2 0.7
2	6	10	1200 1225 1250	58.9 57.9 56.9	11.8 11.5 11.3	-0.4 -0.06 0.2
3	6	12	1050 1075 1100 1200	62.4 60.9 59.4 54.1	11.1 10.5 10.3 9.4	-0.6 -0.1 0.3 1.6
4	10	8	1400 1500 1650 1700	40.2 38.4 36.1 35.4	9.4 9.0 8.9 8.6	-1.3 -0.7 -0.1 0.04
5	10	10	1300 1350 1400	39.5 38.4 37.4	8.0 7.8 7.7	-0.3 -0.06 0.19
6	10	12	1100 1150 1200	40.0 38.5 37.1	7.0 6.6 6.5	-0.2 0.1 0.4
7	14	8	1400 1500 1600 1700 1800 1900	26.9 25.8 24.8 23.9 23.1 22.3	5.0 4.9 4.86 4.7 5.0 4.8	-0.7 -0.55 -0.37 -0.21 -0.1 0.02
8	14	10	1200 1300 1400 1450	26.0 24.6 23.4 22.9	4.4 4.1 4.0 3.8	-0.46 -0.2 -0.02 0.06
9	14	12	1000 1100 1200	23.5 21.8 20.5	3.0 2.8 2.73	-0.19 0.02 0.17

Table 6.1 Results for all the initial positions

Figures 6.1 and 6.2 show the *time of travel vs torque* curves for initial position (6,8) and (10,8) of center of mass respectively. The behavior for the rest of the initial positions is similar to these. Time of travel for all initial positions decreases with increase in the torque at joint 2. In Figure 6.1, the time of travel seems to level at higher torque, indicating that time of travel might be a constant with increase in T_2 beyond 1500 gm-cm/sec^2. However, this is not true. Increasing T_2

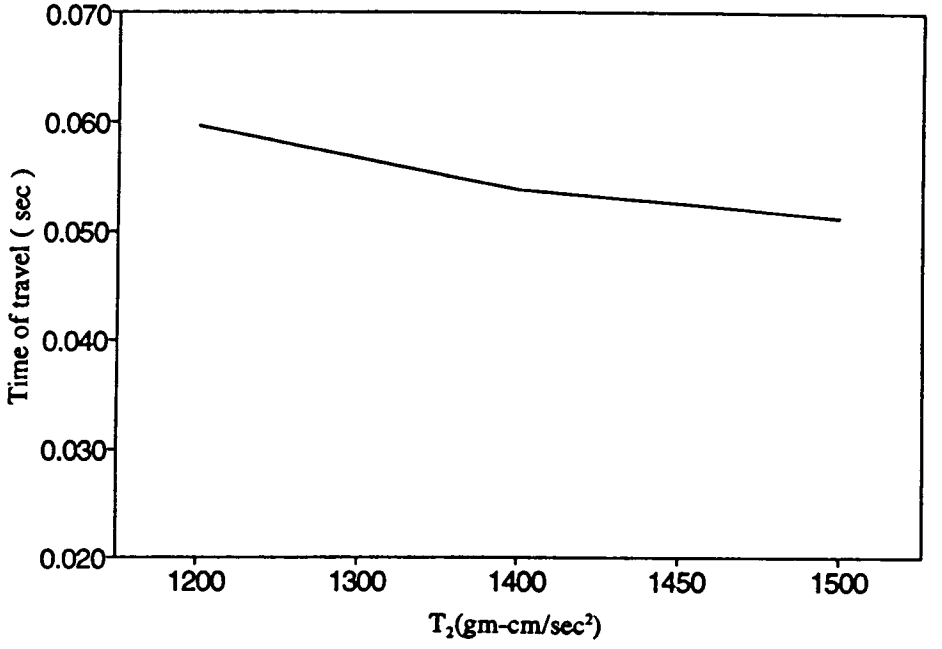

Fig 6.1 Time of travel vs T_2 for initial position (6,8)

beyond 1500gm-cm/sec$_2$ decreases time of travel very much, and thus, higher values of T_2 are not shown in the figure.

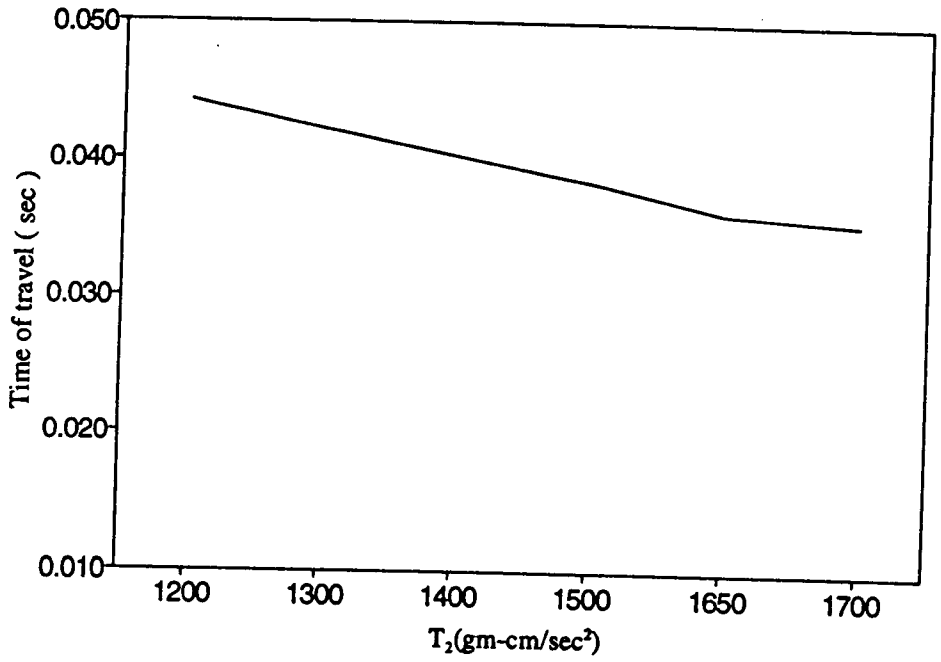

Fig 6.2 Time of travel vs T_2 for initial position (10,8)

Figures 6.3 and 6.4 show the *xtravel vs torque* curves for initial positions (6,8) and (10.8) of center of mass respectively. The behavior is similar for other initial positions. Similar to the time of travel, xtravel decreases with increase in the torque at joint 2. Thus,

higher torque need not necessarily improve the performance of the system. In Figure 6.3, the xtravel appears to level at higher torque. But, similar to the time of travel, the xtravel decreases drastically, at higher T_2. Thus, higher values of T_2 were neglected and not shown in the figure.

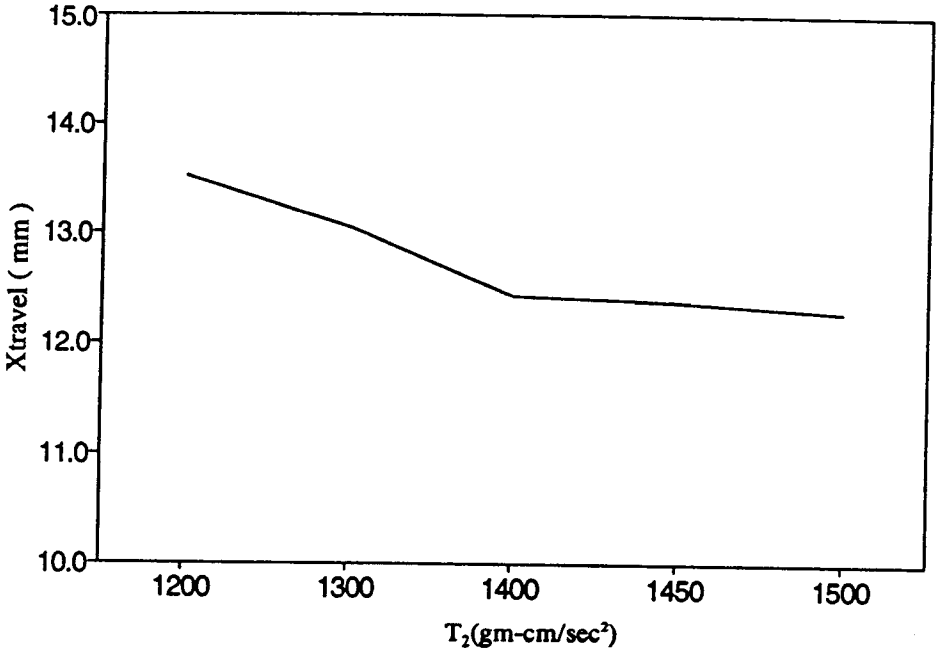

Fig 6.3 Xtravel vs T_2 for initial position (6,8)

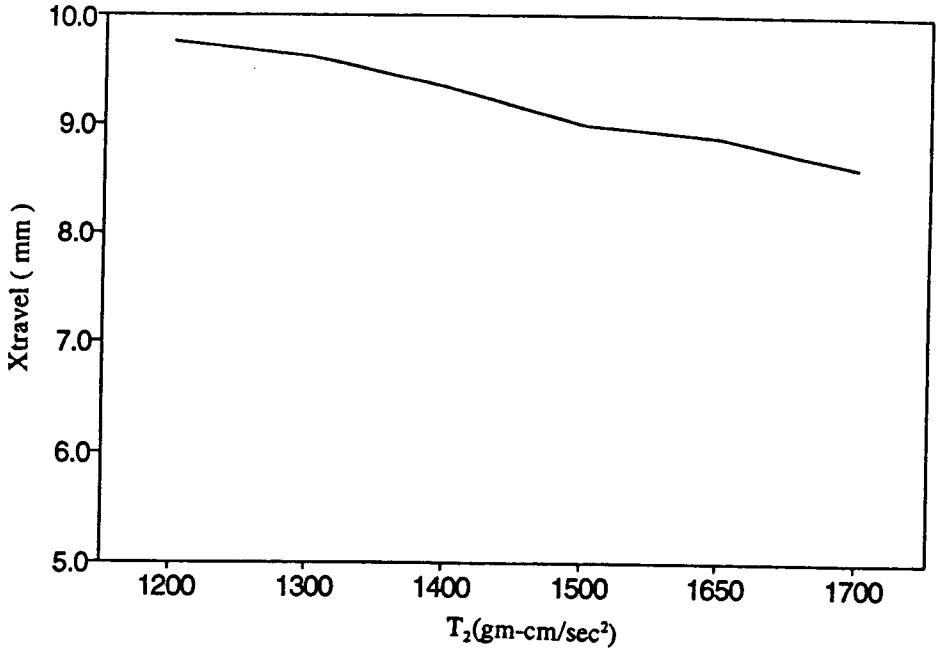

Fig 6.4 Xtravel vs T_2 for initial position (10,8)

Figures 6.5 and 6.6 show the *ytravel vs torque* curves for initial positions (6,8) and (10,8) of center of mass respectively. The behavior for the rest of the initial positions is similar. The ytravel, unlike time of travel and xtravel, increases with increase in the torque at joint 2. However, the ytravel crosses zero for a certain torque, the threshold value. For torques below and above this threshold value, ytravel is of considerable magnitude. However, close to that threshold value of torque, ytravel is either zero or close to zero.

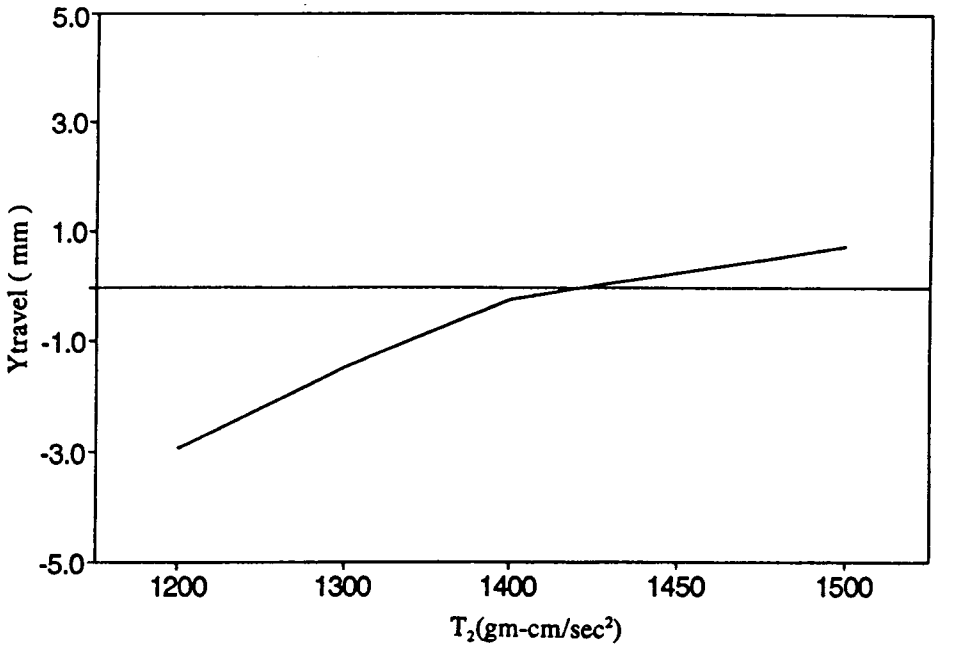

Fig 6.5 Ytravel vs T_2 for initial position (6,8)

The criterion for deciding a good value of torque for a given initial position is based on ytravel. As mentioned before, a ytravel of close to zero is desirable. Thus, the values of the torque at joint 2 resulting in ytravel of zero or close to zero are used to construct tables of initial position versus xtravel to evaluate the behavior of the system.

A very good way of understanding the relationship between the various parameters for the model is by making tables similar to Table 6.2. The values at the bottom

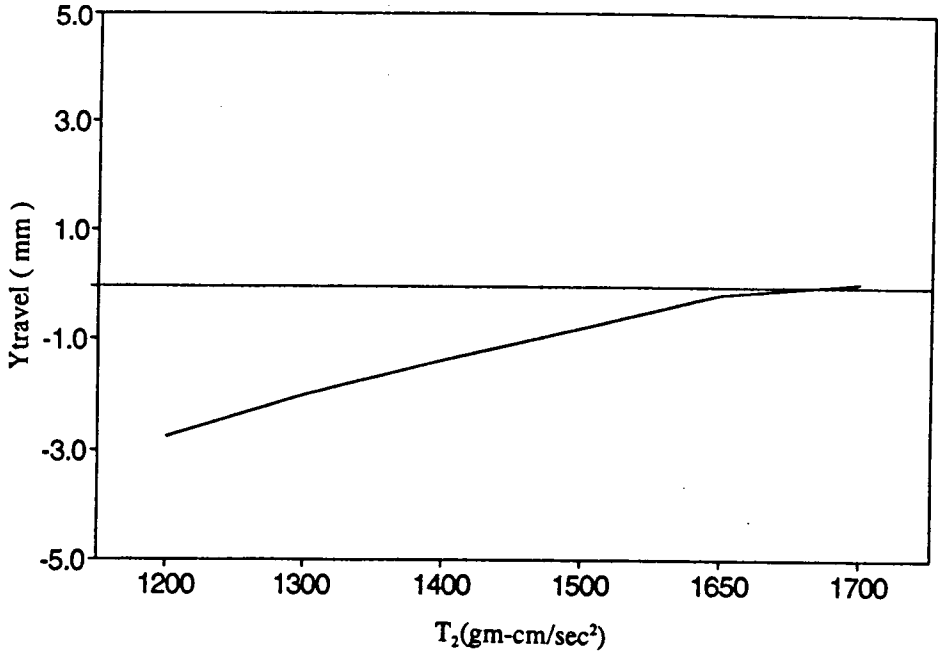

Fig 6.6 Ytravel vs T_2 for initial position (10,8)

indicate the x-coordinate of center of mass, and values on y-axis indicate the y-coordinate of center of mass. The values in the table are for the particular parameter of interest for that initial position. Thus, one can observe the behavior of the system with increase or decrease in the x-coordinate, or the y-coordinate, or both.

The major factors in deciding whether an initial position is good or not are the torque needed at joint 2 and the xtravel. The results for a ytravel of approximately zero, i.e., a ytravel of 0 ± 0.2mm, are

summarized in Tables 6.2, 6.3 and 6.4. The torque needed per unit xtravel gives us an estimate of the efficiency of the system for the given initial position.

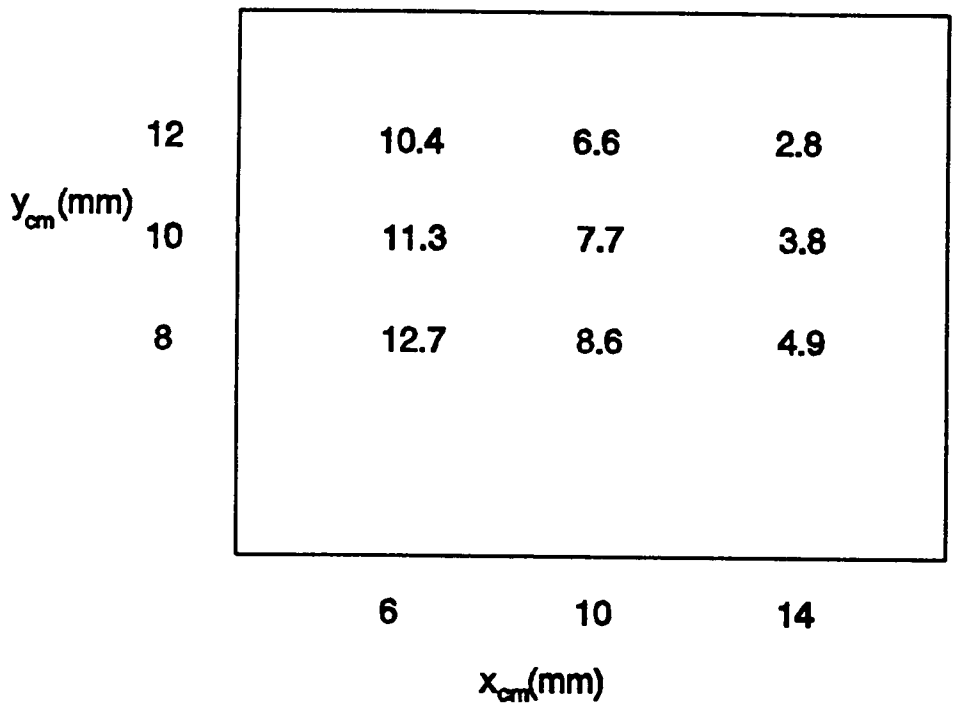

Table 6.2 xtravel for zero ytravel

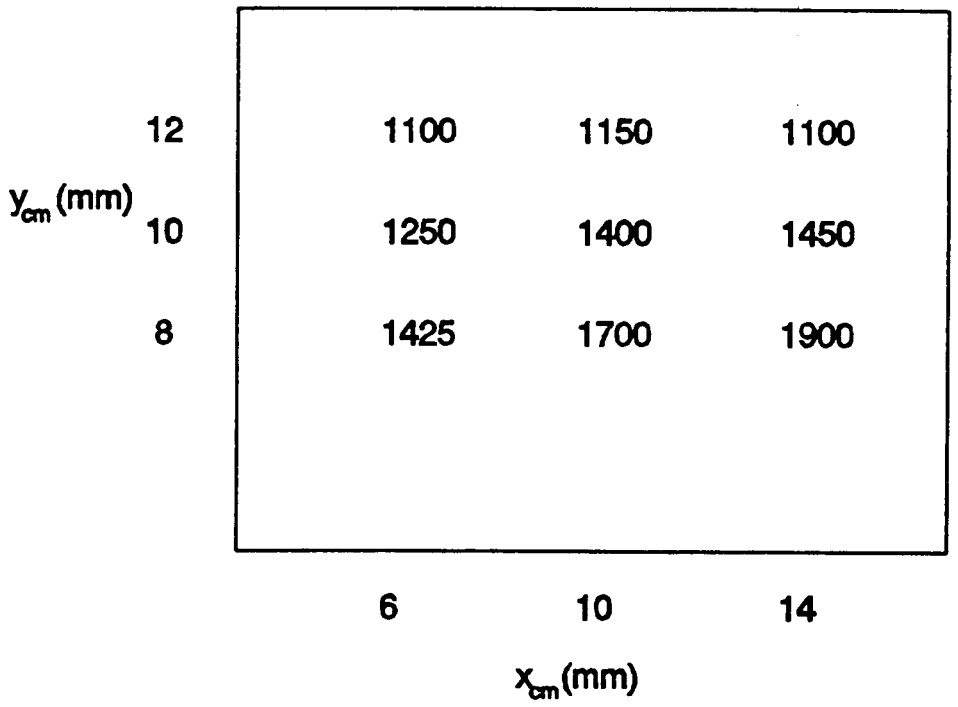

Table 6.3 T_2 for zero ytravel

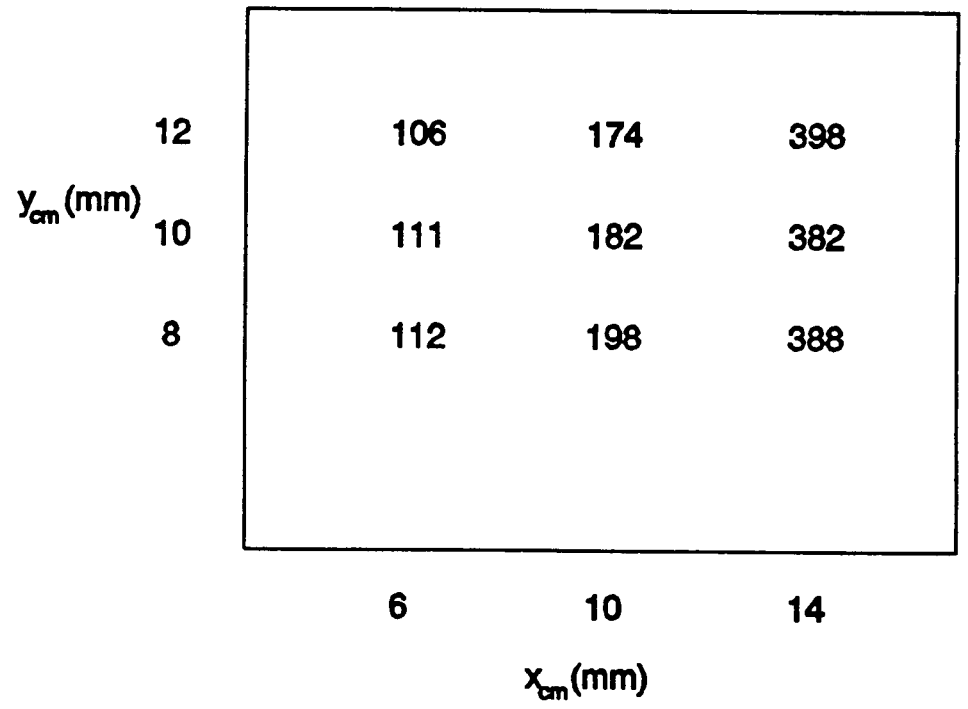

Table 6.4 T_2/mm (unit-T_2) for the two link model

xtravel

As seen from Table 6.2, xtravel decreases with increase in both x and y co-ordinates of the center of mass. Increase in x_{cm} reduces xtravel faster than increase in y_{cm}. For every 4mm increase in x_{cm}, the reduction in xtravel is almost twice as much as for the same increase in y_{cm}.

T_2

As seen from Table 6.3 , The torque needed at joint 2 for a flat trajectory, i.e., with a small ytravel increases with increase in x_{cm} and decreases with an increase in the body height (y_{cm}). The reduction in T_2 with increasing x_{cm}, decreases as the body height increases. At a body height of 12mm, T_2 is almost the same regardless of the value of x_{cm}. At greater body heights, x_{cm} does not influence the torque needed at joint 2 as much as at lower body heights.

T_2 / xtravel (unit-T_2)

The amount of torque needed at joint 2 per unit xtravel gives us an indication of the efficiency of the leg for that initial position. Table 6.4 shows the torque needed per unit xtravel for each of the initial positions. Unit-T_2 increases with increase in x_{cm}. However, for each of the x_{cm}, the unit-T_2 value is almost the same for all

heights. The difference is so small that they can be considered equal. Thus, it is more efficient at lower x_{cm} and body height does not affect the efficiency.

This model does not represent the beetle very well since, in reality the body center-of-mass is not at the place where the hind leg is connected to the body. It is 2.2mm from this joint. However, considerable xtravel and time of travel were observed for this model.

7. ANALYSIS FOR THE THREE LINK MODEL

This chpater discusses the results for the three link model. As mentioned in chapter 2, the paramters analysed are i) Trajectory ii) Time of travel iii) Travel in the x - direction of center of mass (xtravel) and iv) Travel in the y - direction of center of mass (ytravel). Though the program calculates linear velocity of center of mass, it was not considered in the present analysis for same reasons as in chapter 6.

Constraints

As discussed in the two link model analysis, not all the information we get from integrating the equations of motion is useful. Thus, some constraints are put to cut down the unnecessary data. The constraints on the three link model are

1. θ_1 : $0° <= \theta_1 <= 180°$ deg.
2. θ_2 : $0° <= \theta_2 <= 180°$ deg.
3. Height of center of mass: The height of center of mass must always be greater than zero, i.e., above ground level.
4. θ_3 : constant. The value of θ_3 must be a constant,

i.e., the third link must not have any movement with respect to the second link.

As long as the torque needed to support joint 3 is smaller than the friction torque, third link will not move with respect to the second link, i.e., the velocity and acceleration of θ_3 are zero. But, once the torque needed to support joint 3 exceeds the friction torque at that joint, the third link will start moving with respect to the second link.

In the program, as soon as any of the above constraints are violated, the numerical integration is stopped and the data is stored in output files.

Additional foot positions

Foot positions in addition to the ones considered in the two-link model are considered for this model. After looking at the results for the previous foot positions, I wanted to look at some of the intermediate positions for a better understanding of the behaviour of the model. These positions are given in Figure 7.1.

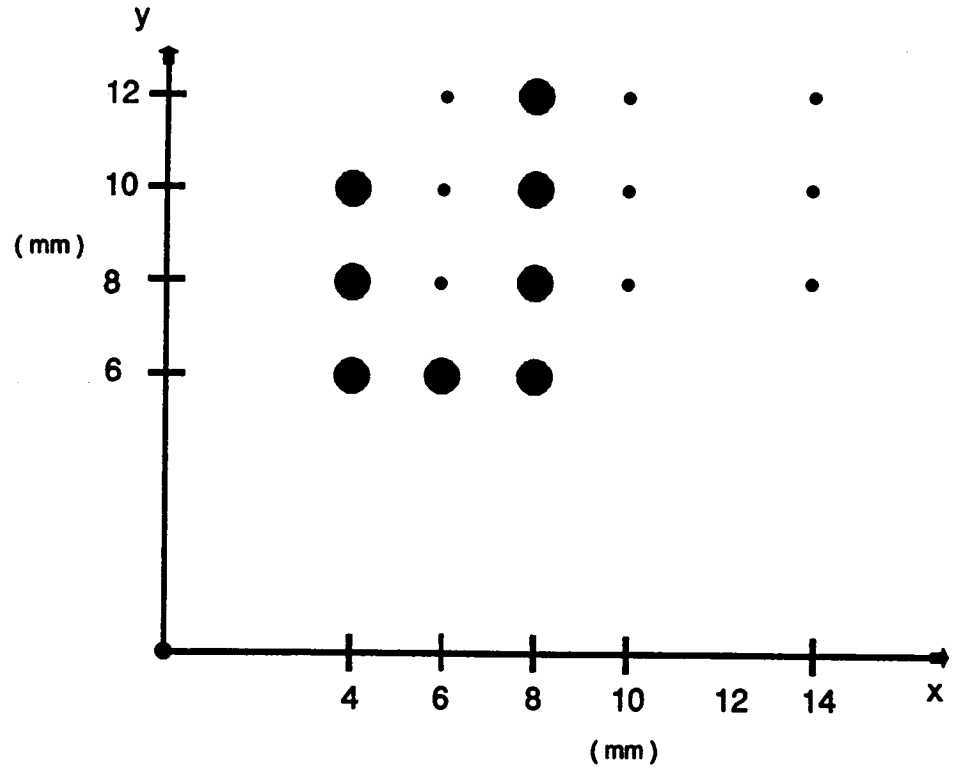

Fig 7.1 Additional positions of center of mass of beetle shown as large dots

Results of the output runs:

For each of the initial positions, the value of T_2 is varied until the required trajectory, i.e., flat trajectory with ytravel of near zero, i.e., ytravel of 0 ± 0.2mm, is obtained. Tables 7.1 and 7.2 give the results of all the runs for this model. The time of travel,

xtravel and ytravel, when plotted against T_2 give us an understanding of the dynamic behavior of the leg.

Set no.	xcm (mm)	ycm (mm)	T2 (gm-cm/ sec^2)	time of travel (mSec)	xtravel (mm)	ytravel (mm)
1	6	8	1200 1300 1400 1500	35.6 31.9 28.8 26.3	4.0 3.36 2.92 2.68	-1.07 -0.47 -0.09 0.17
2	6	10	1100 1200 1300	39.8 34.0 29.5	4.09 3.33 2.58	-1.21 -0.43 0.03
3	6	12	1100 1150 1200	37.2 33.6 30.6	3.31 2.72 2.32	-0.49 -0.14 0.08
4	10	8	1500 1600 1700 1800	17.7 16.5 15.4 14.5	1.56 1.47 1.37 1.26	-0.17 -0.08 -0.001 0.05
5	10	10	1200 1300 1400 1500	22.2 19.9 18.0 16.5	1.98 1.59 1.54 1.30	-0.42 -0.18 -0.05 0.04
6	10	12	1100 1200 1300	23.2 20.3 18	1.91 1.57 1.37	-0.34 -0.10 0.05
7	14	8	1600 1700 1800	11.6 10.9 10.3	0.87 0.76 0.80	-0.10 -0.05 -0.02
8	14	10	1300 1400 1500	13.5 12.4 11.5	0.98 0.89 0.80	-0.12 -0.06 -0.01
9	14	12	1100 1200 1300	14.7 13.2 12.1	0.97 0.90 0.84	-0.13 -0.04 0.015

Table 7.1 Results for the runs for original 9 initial positions

set no	x_{in} (mm)	y_{in} (mm)	T_2 (gm-cm/ sec^2)	Time of travel (mSec)	xtravel (mm)	ytravel (mm)
10	4	6	1200 1300 1400	47.3 44.0 41.0	6.9 6.5 5.7	-2.2 -1.2 -0.3
11	4	8	1100 1200 1300 1350	52.0 46.2 40.9 38.6	6.6 5.4 4.3 4.0	-2.5 -1.0 -0.06 0.24
12	4	10	1200 1225 1250 1300	43.6 41.6 39.8 36.6	3.9 3.6 3.3 2.9	-0.15 0.05 0.22 0.47
13	6	6	1300 1500 1600 1700	33.3 28.8 27.0 25.3	4.4 3.6 3.5 3.2	-1.28 -0.39 -0.14 0.09
14	8	6	1600 1700 1800 1900	21.2 19.9 18.8 17.8	2.4 2.1 2.0 1.9	-0.35 -0.18 -0.07 0.01
15	8	8	1400 1500 1600	23.3 21.4 19.8	2.3 2.1 1.8	-0.29 -0.10 0.04
16	8	10	1200 1300 1400	27.2 24.1 21.6	2.6 2.2 1.8	-0.47 -0.15 0.05
17	8	12	1200 1250 1300	24.8 23.2 21.7	1.9 1.8 1.5	-0.06 0.06 0.14

Table 7.2 Results for additional foot positions for three link model

Increasing friction torque

Increasing the friction torque at joint 3, increases the stiffness of this joint. As friction torque, t_f,

approaches inifinity, the three link model should behave as the two link model. Thus, few runs were made for initial position (6,8) to check this. The results are shown in Table 7.3.

x_{in} (mm)	y_{in} (mm)	T_2 (gm-cm/ sec^2)	t_r (gm-cm/ sec^2)	time of travel (mSec)	xtravel (mm)	ytravel (mm)
6	8	1400	10	28.8	2.92	-0.09
6	8	1400	20	34.1	4.41	-0.19
6	8	1400	40	40.6	6027	-0.36
6	8	1400	60	44.7	7.74	-0.52
6	8	1400	80	47.6	8.97	-0.67
6	8	1400	100	49.8	9.86	-0.78

Table 7.3 Results for different friction torque values for initial position (6,8)

Time of travel and xtravel increase with increase in friction torque at joint 3. For friction torque of 100gm-cm/sec2, xtravel is close to 10mm. This is close to the value 12.4mm of xtravel, from Table 6.1, obtained for the two link model for this initial position.

Plots

Figures 7.2 & 7.3 show the *Time of travel vs torque* curves for initial position (6,8) and (10,8). The behaviour for the rest of the initial positions is similar to these. The time of travel for all the initial positions decreases with increase in torque at joint 2.

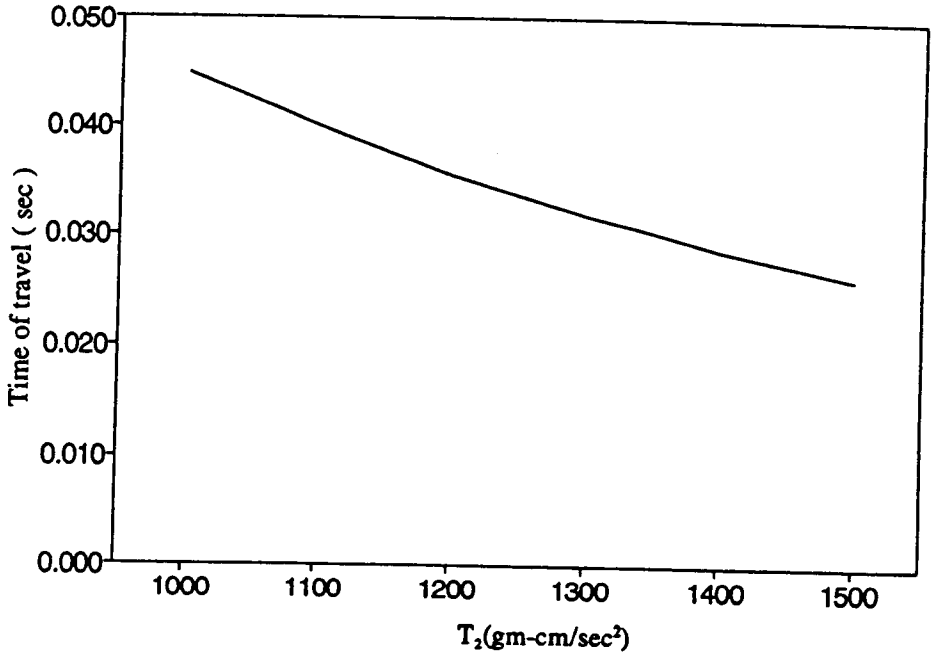

Fig 7.2 Time of travel vs T_2 for initial position (6,8)

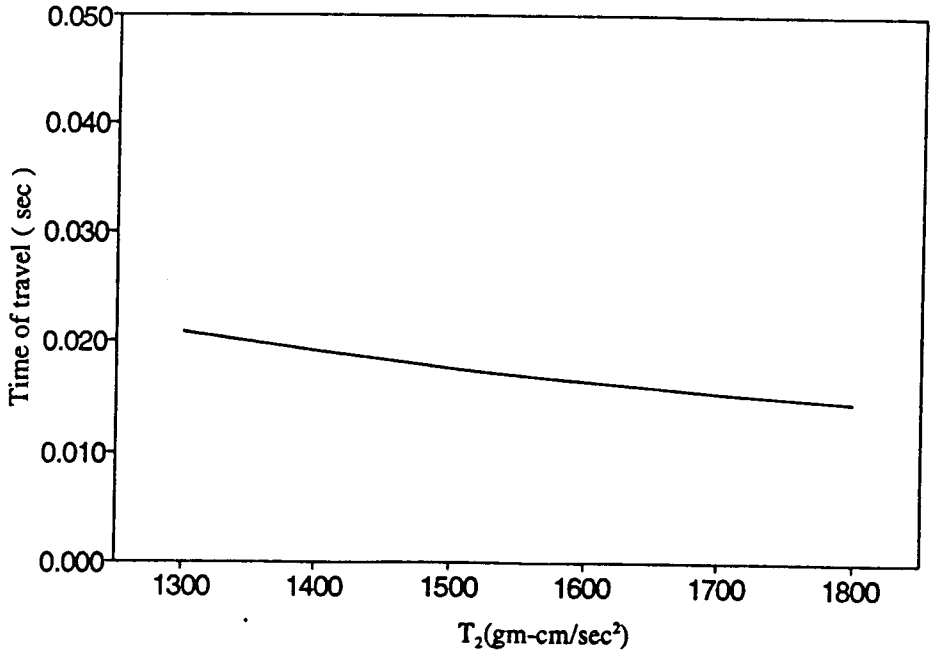

Fig 7.3 Time of travel vs T_2 for initial position (10,8)

The time of travel seems to level at higher T_2, in Figure 7.2. But, further increase in torque decreased the time of travel very much. and thus, higher values of T_2 were not shown in the figure.

Figures 7.4 and 7.5 show the *xtravel vs torque* curves for initial positions (6,8) and (10,8) respectively. Similar behavior is observed for other initial positions. Similar to the time of travel, xtravel decreases with increase in the torque at joint 2. Thus, higher torque need not necessarily improve the performance of the

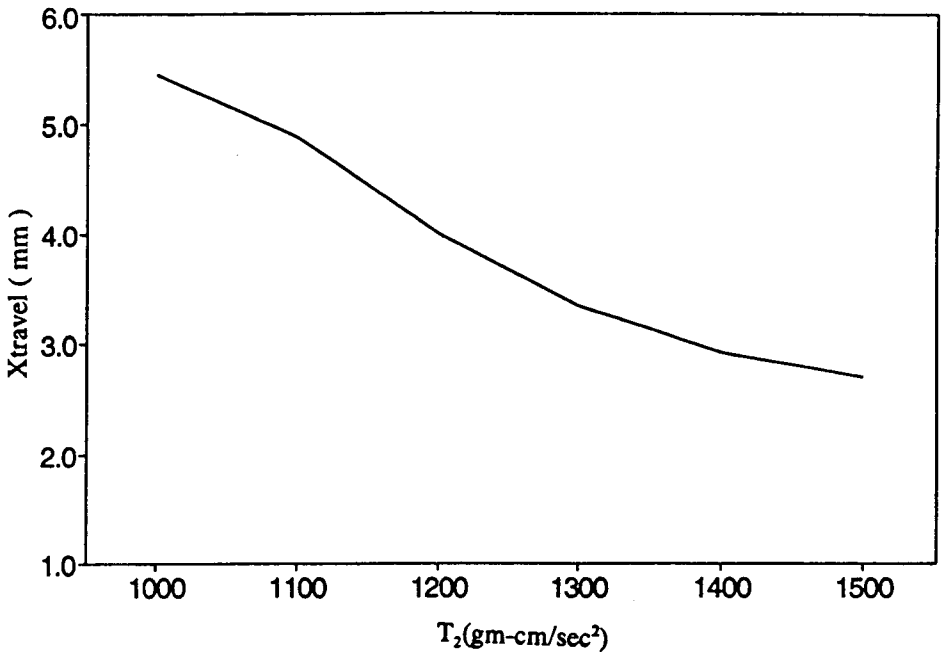

Fig 7.4 Xtravel vs T_2 for initial position (6,8)

system. The xtravel decreased drasticslly at higher T_2. Thus, higher values of T_2 were not shown in the figure.

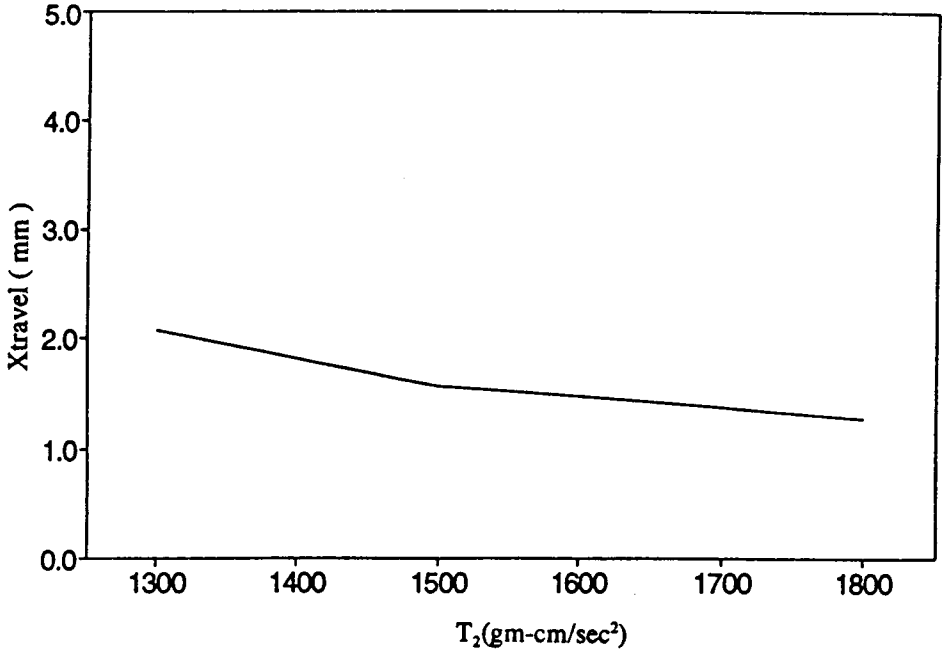

Fig 7.5 Xtravel vs T_2 for initial position (10,8)

Figures 7.6 and 7.7 show the *ytravel vs torque* curves for initial positions (6,8) and (10,8) respectively. Behavior for the rest of the initial positions is similar. The ytravel, unlike time of travel and xtravel, increases with increase in torque at joint 2. However, the ytravel crosses zero for a certain torque, the threshold value. For torques below and above this threshold value, the travel is going to be of considerable magnitude. However, close to that threshold value of torque, the ytravel is either zero or close to zero.

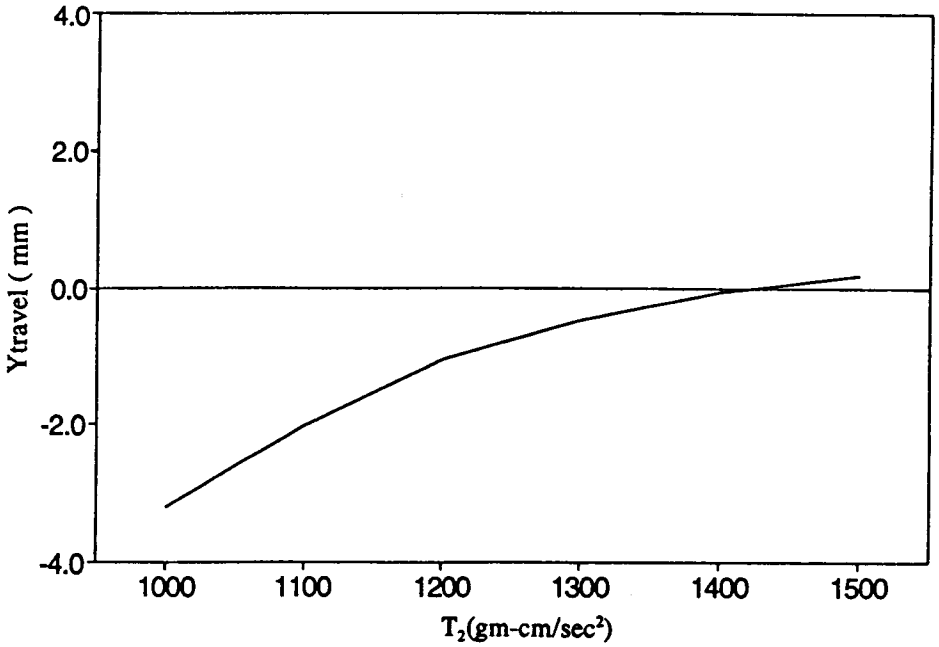

Fig 7.6 Ytravel vs T_2 for initial position (6,8)

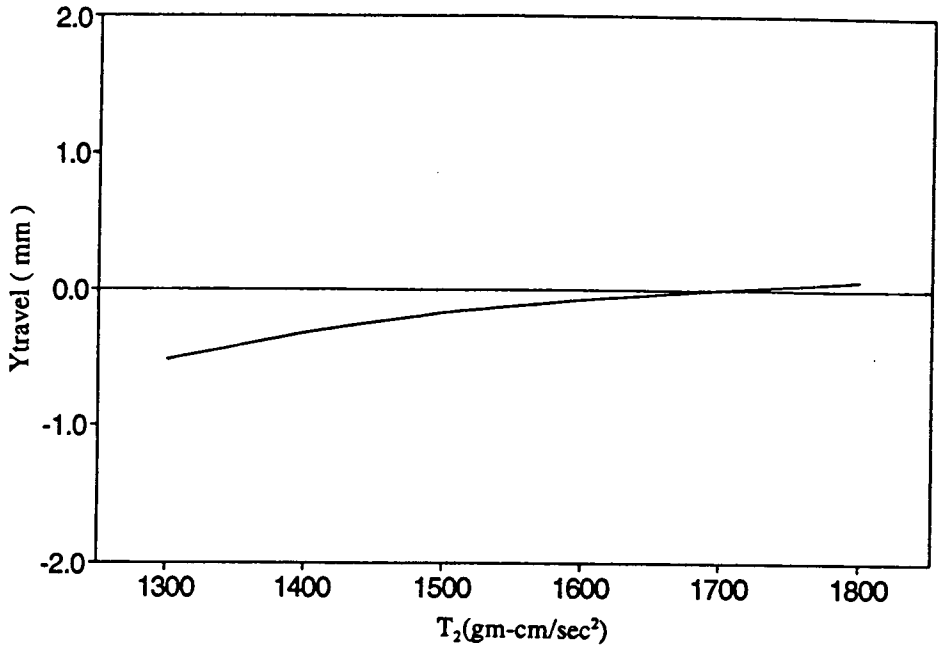

Fig 7.7 Ytravel vs T_2 for initial position (10,8)

As explained in chapter 6, the criterion for deciding a good value of torque for a given initial position is based on ytravel. As mentioned before, a ytravel of close to zero, i.e., ytravel of 0 ± 0.2mm, is desirable. Thus, values of torque at joint 2 and xtravel, resulting in a ytravel of close to zero are used to construct tables of initial positions versus xtravel to evaluate the behavior of the system.

The values at the bottom of Table 7.4 are the initial

x-coordinates of center of mass and values on y-axis are the initial y-coordinate of center of mass. The values in the table are for the particular parameter of interest for that initial possition. Thus, one can observe the behavior of the system with increase or decrease in the x-coordinate, or the y-coordinate, or both.

The major factors in deciding whether an initial position is good or not are the torque needed at joint 2 and the xtravel. The results for a ytravel of approximately zero are summarized in tables 7.4, 7.5, and 7.6. The torque needed per unit xtravel gives us an estimate of the efficiency of the system for the given initial position.

y_{cm}(mm) \ x_{cm}(mm)	4	6	8	10	14
12	--	2.3	1.8	1.4	0.85
10	3.6	2.6	1.8	1.3	0.8
8	4.0	2.8	1.8	1.3	0.7
6	--	3.2	1.9	--	--

Table 7.4 xtravel for zero ytravel for three link model

y_{cm}(mm) \ x_{cm}(mm)	4	6	8	10	14
12	---	1200	1250	1300	1300
10	1225	1300	1400	1500	1550
8	1350	1450	1600	1800	1900
6	---	1700	1900	---	---

Table 7.5 T_2 for zero ytravel for three link model

y_{cm}(mm) \ x_{cm}(mm)	4	6	8	10	14
12	---	522	698	950	1545
10	340	500	782	1154	1867
8	340	518	884	1430	2715
6	---	531	1000	---	---

Table 7.6 unit-T_2 for three link model

xtravel

As seen from Table 7.4, xtravel decreases with increase in the x-coordinate of center of mass (x_{cm}). The xtravel also decreases with increase in y-coordinate of center of mass (y_{cm}) for x_{cm} of 4mm, 6mm and 8mm. However, for x_{cm} of 10mm and 14mm, xtravel increases with increase in y_{cm}. A reasonably flat trajectory could not be found for initial position (4,6), i.e., magnitude of ytravel was more than 0.2mm. The model collapses for T_2 values of more than 1400. Thus, I concluded that this position is not stable. I included this in the table to indicate that there is a high xtravel for this position and yet is not a suitable position.

The difference in xtravel with increase in y_{cm}, for each of the x_{cm}, is small. This gives an indication that body height does not influence the xtravel very much. However, x_{cm} influences the xtravel considerably. Lower the value of x_{cm}, the better is the value of xtravel. However, at x_{cm} of 4mm is not a suitable position at lower body heights such as 6mm or lower, indicating that decreasing the x_{cm} does not help after a certain value, 4mm in this case.

T2

As seen from Table 7.5, the torque needed at joint 2 for a flat trajectory, i.e., with a ytravel of near zero,

increases with increase in x_{cm} for all the body heights, i.e., y_{cm} of 6, 8, 10, and 12 mm. However, the magnitude of increase, decreases with increase in the y_{cm}. The difference in T_2 with increasing x_{cm}, decreases as the body height increases. At a body height of 12mm, T_2 is almost the same regardless of the value of x_{cm}. For a given value of x_{cm}, the value of T_2 decreases with an increase in the body height.

This gives an indication that it requires less torque at higher body heights and lower x_{cm}.

T_2 / xtravel (unit-T_2)

The amount of torque needed at joint 2 per unit xtravel gives us an indication of the efficiency of the leg for that initial position. Table 7.6 shows the torque needed per unit xtravel for each of the initial positions.

As seen from Table 7.6, unit-T_2 increases with increase in x_{cm}. However, it decreases with increase in body height for x_{cm} of 6, 8, 10, and 14mm. For x_{cm} of 4mm, however, it increases. Though, the value of unit-T_2 is very low for initial position of (4,6), it is not very useful because this did not result in a flat trajectory. The unit-T_2 is less at higher body heights for each of the x_{cm} discussed.

Thus it gives an indication that it is more efficient

at higher body heights with minimum for initial position (6,10), i.e., x_{cm} of 6mm and a body height of 10mm.

Looking at the xtravel for two link and three link models, we notice that xtravel for the three link model is very short compared to the two link model. Maximum xtravel obtained for a flat trajectory for the three link model is 4.0mm, for initial position (4,8). The maximum xtravel for the two link model is 12.7. Baek(1990) found that the stride length of the beetle is about 12mm. This indicates that the present three link model does not represent the beetle very well.

8. CONCLUSIONS AND SUGGESTIONS FOR FUTURE STUDY

The main objective of this thesis was to find some general patterns in the behavior of motion of the beetle with respect to initial position of the hind leg. Conclusions from this study are as follows.

1. Body height does not affect the motion of the model very much.
2. The x_{cm} plays a significant role. Lower the x_{cm}, the better are xtravel and torque per unit xtravel.
3. Xcm of lower than 6mm is unstable at lower body heights.

The study of dynamics of walking of a beetle is still under development, and a number of aspects in this area require further attention. This chapter includes recommendations for future study of selected areas related to the subject of this thesis.

Only two dimensional models are studied for this thesis. A three dimensional model represents the beetle much better and this would also help in building an actual robot based on this model. Studying the three dimensional model would give us a better understanding of the walking mechanism of a beetle. Since animal is symmetrical, this might not be true for a straight line push off in the forward direction. But, for other directions, study of three dimensional model is would be more useful.

Only nine initial positions were studied for the two-link model

and only seventeen initial positions were studied for the three-link model. Additional foot positions should be subjected to further study.

For the three-link model, constant friction torque was considered at joint 3. At present we have no information about the torque at this joint. Instead of friction torque, a torque based on the muscle characteristics would be more appropriate. Further study in this area would help in controlling the trajectory of the center of mass of beetle.

For both two-link and three-link models, constant torque was considered at joint 2. However, a variable torque based on muscle characteristics would enable us to control the trajectory. This would also improve xtravel and time of travel.

A model based on the combined hind and middle legs can be developed. The body connecting these two legs could be considered a rigid link. Unlike the models considered in this thesis, this would form a closed loop mechanism. So far lifting a foot off the ground has not been considered. With the proposed model even this could be studied.

Finally, the Runge-Kutta numerical integration algorithm used for this thesis uses a constant time step. Using a variable time step would reduce the processing time without sacrificing the accuracy. The current function performing the numerical integration, could be replaced by a variable step size numerical integration procedure.

BIBLIOGRAPHY

Albright, S.L., 1990. Kinematics of Arthropod Legs: Modelling and Measurement. Ph.D. thesis, Oregon State University.

Baek, Y.S., 1990. Kinematic Analysis of Legged System Locomotion on Smooth Horizontal Surfaces. Ph.D. thesis, Oregon State University.

Craig, J.J., 1986. Introduction to Robotics. Addison Wesley, pp.

Fichter, E.F., Fichter, B.L. and Albright S.L., 1987. Arthropods: 350 Million Years of Successful Walking Machine Design. Proceeding of the Seventh World Congress on the Theory of Machines and Mechanisms, Sevilla, Spain, September, pp. 1877-1880.

Gewecke, M. and Wendler, G., 1985. Insect Locomotion. Paul Parey, pp. 1-102.

Kane, Thomas R., Levinson, David A., 1985. Dynamics, Theory and Applications. McGraw-Hill.

Pedley, T.J., 1977. Scale Effects in Animal Locomotion. Academic Press.

Press, William H., 1988. Numerical Recipes in C: The Art of Scientific Computing. Cambridge University Press.

Song, S.M. and Waldron, K.J., 1989. Machines That Walk. The MIT Press.

Todd, D.J., 1985. Walking Machines: An Introduction to Legged Robots, Chapman and Hall.

APPENDICES

APPENDIX A

DERIVATIONS FOR INCORPORATING FRICTION TORQUE AND FOR LINEAR VELOCITY OF CENTER OF MASS

A.1 Initial position for 2 link model

Given the x and y coordinates of the center of mass with respect to the foot, there is a need to calculate the initial orientation of the two links. Figure A.1.1 shows the initial orientation of the two-link model.

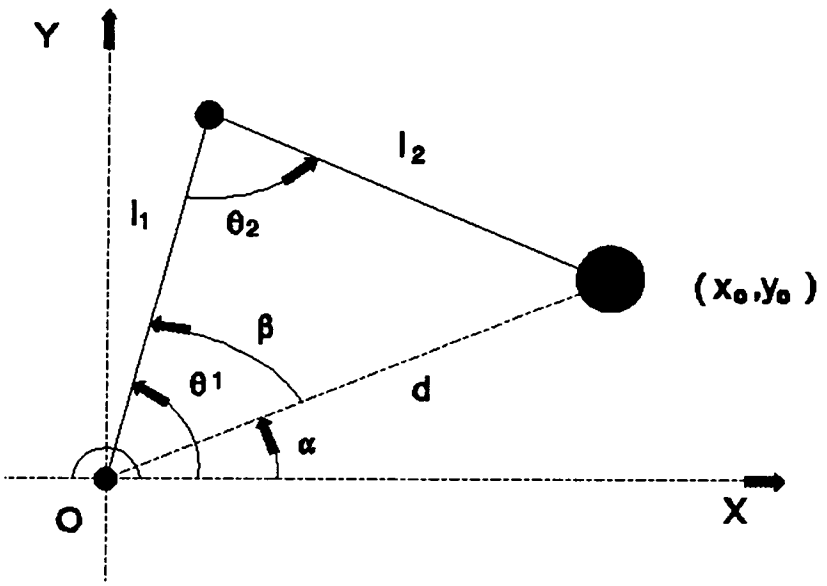

Fig A.1.1 Initial position for two link model

The initial position x_o, y_o and the lengths l_1 and l_2 are known.

$$d_2 = x_o^2+y_o^2 = l_1^2+l_2^2-2l_1l_2\cos\theta_2$$

$$\therefore \theta_2 = \cos^{-1}\left(\frac{l_1^2+l_2^2-d^2}{2l_1l_2}\right)$$

$$\alpha = \cos^{-1}\left(\frac{l_1^2+d^2-l_2^2}{2l_1d}\right) \quad \text{and} \quad \beta = \tan^{-1}\left(\frac{Y_0}{X_0}\right)$$

$$\theta_1 = \alpha+\beta = \cos^{-1}\left(\frac{l_1^2+d^2-l_2^2}{2l_1d}\right) + \tan^{-1}\left(\frac{Y_0}{X_0}\right)$$

Thus, the initial values for the generalized coordinates θ_1 and θ_2 are described.

A.2 Initial position for 3 link model

For our analysis, it is assumed that the x_c and y_c, the coordinates of the center of mass, and the orientation of the third link are known. From these values it is necessary to find the three generalized coordinates θ_1, θ_2 and θ_3, shown in Figure A.2.1. For this analysis, the orientation of the third link is assumed to be the line joining the foot and the center of mass. Figure A.2.1 describes the system.

$$\gamma = \theta_1+\theta_2+\theta_3-\pi$$

as α, x_c, y_c, l_1, l_2 and l_3 are known,

$x_o = x_c - l_3\cos\gamma$ and $y_o = y_c - l_3\sin\gamma$

$\gamma = \tan^{-1}(y_c/x_c)$

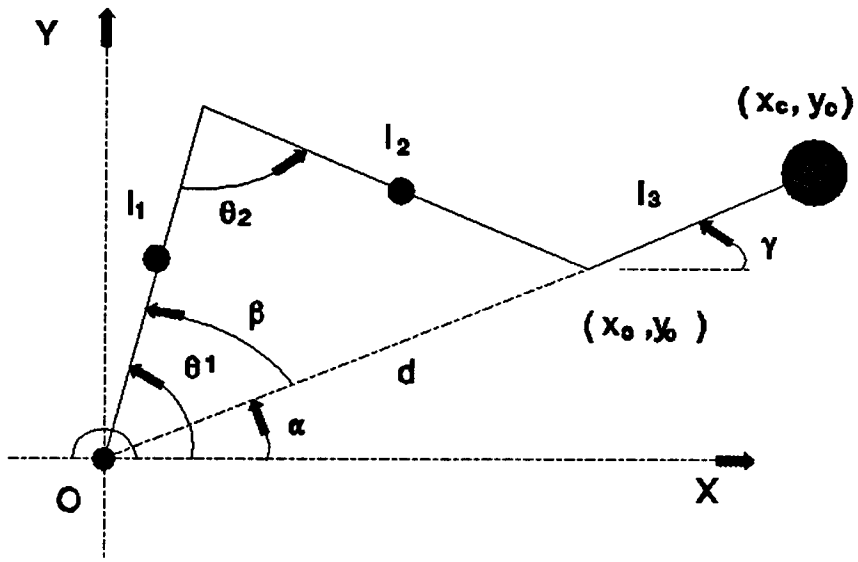

Fig A.2.1 Initial position for three link model

Now that we have calculated x_o and y_o, the rest of the calculations are similar to the two-link problem given in appendix A.1. Thus,

$d_2 = x_o^2 + y_o^2$

$$\theta_1 = \cos^{-1}\left(\frac{l_1^2+d^2-l_2^2}{2l_1d}\right) + \tan^{-1}\left(\frac{y_o}{x_o}\right)$$

$$\theta_2 = \cos^{-1}\left(\frac{l_1^2+l_2^2-d^2}{2l_1l_2}\right)$$

$$\theta_3 = \gamma+\pi-(\theta_1+\theta_2)$$

Thus, the initial values for the generalized coordinates θ_1, θ_2 and θ_3 are described.

A.3 Rearranging equations for three-link model

The expressions for T_1, T_2 and T_3 can be rewritten as,

$$a_1\ddot{\theta}_1+a_2\ddot{\theta}_2+a_3\ddot{\theta}_3 = T_1-a_4\dot{\theta}_1^2-a_5\dot{\theta}_2^2-a_6\dot{\theta}_3^2-a_7\dot{\theta}_1\dot{\theta}_2-a_7\dot{\theta}_2\dot{\theta}_3-a_7\dot{\theta}_3\dot{\theta}_1-a_{10}$$

$$b_1\ddot{\theta}_1+b_2\ddot{\theta}_2+b_3\ddot{\theta}_3 = T_2-b_4\dot{\theta}_1^2-b_5\dot{\theta}_2^2-b_6\dot{\theta}_3^2-b_7\dot{\theta}_1\dot{\theta}_2-b_8\dot{\theta}_2\dot{\theta}_3-b_9\dot{\theta}_3\dot{\theta}_1-b_{10}$$

$$c_1\ddot{\theta}_1+c_2\ddot{\theta}_2+c_3\ddot{\theta}_3 = T_3-c_4\dot{\theta}_1^2-c_5\dot{\theta}_2^2-c_6\dot{\theta}_3^2-c_7\dot{\theta}_1\dot{\theta}_2-c_8\dot{\theta}_2\dot{\theta}_3-c_9\dot{\theta}_3\dot{\theta}_1-c_{10}$$

They can also be written as,

$$\begin{bmatrix} a_1 & a_2 & a_3 \\ b_1 & b_2 & b_3 \\ c_1 & c_2 & c_3 \end{bmatrix} \begin{bmatrix} \ddot{\theta}_1 \\ \ddot{\theta}_2 \\ \ddot{\theta}_3 \end{bmatrix} = \begin{bmatrix} T_1-a_{10} \\ T_2-b_{10} \\ T_3-c_{10} \end{bmatrix} - \begin{bmatrix} a_4 & a_5 & a_6 \\ b_4 & b_5 & b_6 \\ c_4 & c_5 & c_6 \end{bmatrix} \begin{bmatrix} \dot{\theta}_1^2 \\ \dot{\theta}_2^2 \\ \dot{\theta}_3^2 \end{bmatrix} - \begin{bmatrix} a_7 & a_8 & a_9 \\ b_7 & b_8 & b_9 \\ c_7 & c_8 & c_9 \end{bmatrix} \begin{bmatrix} \dot{\theta}_1\dot{\theta}_2 \\ \dot{\theta}_2\dot{\theta}_3 \\ \dot{\theta}_3\dot{\theta}_1 \end{bmatrix} \quad \text{(A.3.1)}$$

Let A be a matrix given by,

$$A = \begin{bmatrix} a_1 & a_2 & a_3 \\ b_1 & b_2 & b_3 \\ c_1 & c_2 & c_3 \end{bmatrix}$$

and let the inverse of this matrix be represented by

$$A^{-1} = \begin{bmatrix} A_{11} & A_{12} & A_{13} \\ B_{11} & B_{12} & B_{13} \\ C_{11} & C_{12} & C_{13} \end{bmatrix}$$

where,

$\det = a_1(b_2c_3-b_3c_2)-b_1(a_2c_3-a_3c_2)+c_1(a_2b_3-a_3b_2)$

$A_{11}=(b_2c_3-b_3c_2)/\det \qquad A_{12}=-(a_2c_3-a_3c_2)/\det$

$A_{13}=(a_2b_3-a_3b_2)/\det \qquad A_{21}=-(b_1c_3-b_3c_1)/\det$

$A_{22}=(a_1c_3-a_3c_1)/\det \qquad A_{23}=-(a_1b_3-a_3b_1)/\det$

$A_{31}=(b_1c_2-b_2c_1)/\det \qquad A_{32}=-(a_1c_2-a_2c_1)/\det$

$A_{33}=(a_1b_2-a_2b_1)/\det$

premultiplying both sides of Equation A.3.1 with matrix A^{-1} would give

$$\begin{bmatrix} \theta_1 \\ \theta_2 \\ \theta_3 \end{bmatrix} = A^{-1}\begin{bmatrix} T_1-a_{10} \\ T_2-b_{10} \\ T_3-c_{10} \end{bmatrix} - A^{-1}\begin{bmatrix} a_4 & a_5 & a_6 \\ b_4 & b_5 & b_6 \\ c_4 & c_5 & c_6 \end{bmatrix}\begin{bmatrix} \theta_1^2 \\ \theta_2^2 \\ \theta_3^2 \end{bmatrix} - A^{-1}\begin{bmatrix} a_7 & a_8 & a_9 \\ b_7 & b_8 & b_9 \\ c_7 & c_8 & c_9 \end{bmatrix}\begin{bmatrix} \theta_1\theta_2 \\ \theta_2\theta_3 \\ \theta_3\theta_1 \end{bmatrix}$$

$$\begin{bmatrix} \theta_1 \\ \theta_2 \\ \theta_3 \end{bmatrix} = \begin{bmatrix} G_1 \\ G_2 \\ G_3 \end{bmatrix} - \begin{bmatrix} A_4 & A_5 & A_6 \\ B_4 & B_5 & B_6 \\ C_4 & C_5 & C_6 \end{bmatrix}\begin{bmatrix} \theta_1^2 \\ \theta_2^2 \\ \theta_3^2 \end{bmatrix} - \begin{bmatrix} A_7 & A_8 & A_9 \\ B_7 & B_8 & B_9 \\ C_7 & C_8 & C_9 \end{bmatrix}\begin{bmatrix} \theta_1\theta_2 \\ \theta_2\theta_3 \\ \theta_3\theta_1 \end{bmatrix} \qquad \text{(A.3.2)}$$

Where, A's, B's, C's and G's are given by,

$A_i = A_{11}a_i+A_{12}b_i+A_{13}c_i \qquad$ for i = 4 to 9

$B_i = A_{21}a_i+A_{22}b_i+A_{23}c_i$ for i = 4 to 9

$C_i = A_{31}a_i+A_{32}b_i+A_{33}c_i$ for i = 4 to 9

$G_i = A_{i1}(T_1-a_{10})+A_{i2}(T_2-b_{10})+A_{i3}(T_3-c_{10})$ for i = 1 to 3

and the angular accelerations of the joints are given by,

$$\ddot{\theta}_1 = G_1-A_4\dot{\theta}_1^2-A_5\dot{\theta}_2^2-A_6\dot{\theta}_3^2-A_7\dot{\theta}_1\dot{\theta}_2-A_8\dot{\theta}_2\dot{\theta}_3-A_9\dot{\theta}_3\dot{\theta}_1 \quad \text{(A.3.3)}$$

$$\ddot{\theta}_2 = G_2-B_4\dot{\theta}_1^2-B_5\dot{\theta}_2^2-B_6\dot{\theta}_3^2-B_7\dot{\theta}_1\dot{\theta}_2-B_8\dot{\theta}_2\dot{\theta}_3-B_9\dot{\theta}_3\dot{\theta}_1 \quad \text{(A.3.4)}$$

$$\ddot{\theta}_3 = G_3-C_4\dot{\theta}_1^2-C_5\dot{\theta}_2^2-C_6\dot{\theta}_3^2-C_7\dot{\theta}_1\dot{\theta}_2-C_8\dot{\theta}_2\dot{\theta}_3-C_9\dot{\theta}_3\dot{\theta}_1 \quad \text{(A.3.5)}$$

Integrating Equations A.3.3, A.3.4 & A.3.5 would give the values of three generalized coordinates and their velocities.

A.4 Incorporating friction torque into the software

Incorporating the friction torque into the software is explained in this section. As explained in chapter 5, friction torque is assumed to be acting at the third joint. The third link will not move until the torque on the third joint exceeds the friction torque.

From chapter 5, Equations 5.11 and 5.12 can be rewritten as,

$$\text{if} \quad \mathbf{A} = \begin{bmatrix} a_1 & a_2 \\ b_1 & b_2 \end{bmatrix} \quad \textit{then,}$$

$$\mathbf{A}^{-1} = \frac{1}{a_1 b_2 - a_2 b_1} \begin{bmatrix} b_2 & -a_2 \\ -b_1 & a_1 \end{bmatrix} = \begin{bmatrix} A_{11} & A_{12} \\ A_{21} & A_{22} \end{bmatrix}$$

and premultiplying both sides with A^{-1} gives

$$\begin{bmatrix} \ddot{\theta}_1 \\ \ddot{\theta}_2 \end{bmatrix} = \mathbf{A}^{-1} \begin{bmatrix} (T_1 - a_{10}) & -a_3 \\ (T_2 - b_{10}) & -b_3 \end{bmatrix} \begin{bmatrix} 1 \\ \ddot{\theta}_3 \end{bmatrix} - \mathbf{A}^{-1} \begin{bmatrix} a_4 & a_5 & a_6 \\ b_4 & b_5 & b_6 \end{bmatrix} \begin{bmatrix} \dot{\theta}_1^2 \\ \dot{\theta}_2^2 \\ \dot{\theta}_3^2 \end{bmatrix} - \mathbf{A}^{-1} \begin{bmatrix} a_7 & a_8 & a_9 \\ b_7 & b_8 & b_9 \end{bmatrix} \begin{bmatrix} \dot{\theta}_1\dot{\theta}_2 \\ \dot{\theta}_2\dot{\theta}_3 \\ \dot{\theta}_3\dot{\theta}_1 \end{bmatrix}$$

the above equation when simplified, can be represented as

$$\ddot{\theta}_1 = G_1 - A_3\ddot{\theta}_3 - A_4\dot{\theta}_1^2 - A_5\dot{\theta}_2^2 - A_6\dot{\theta}_3^2 - A_7\dot{\theta}_1\dot{\theta}_2 - A_8\dot{\theta}_2\dot{\theta}_3 - A_9\dot{\theta}_3\dot{\theta}_1$$

$$\ddot{\theta}_2 = G_1 - B_3\ddot{\theta}_3 - B_4\dot{\theta}_1^2 - B_5\dot{\theta}_2^2 - B_6\dot{\theta}_3^2 - B_7\dot{\theta}_1\dot{\theta}_2 - B_8\dot{\theta}_2\dot{\theta}_3 - B_9\dot{\theta}_3\dot{\theta}_1$$

where,

$A_i = A_{11}a_i + A_{12}b_i$ for i = 3 to 9

$B_i = A_{21}a_i + A_{22}b_i$ for i = 3 to 9

$G_i = A_{i1}(T_1 - a_{10}) + A_{i2}(T_2 - b_{10})$ for i = 1 to 2

then, the torque needed at joint 3 to keep this in constant orientation would be given by,

$$T_3 = c_1\ddot{\theta}_1 + c_2\ddot{\theta}_2 + c_3\ddot{\theta}_3 + c_4\dot{\theta}_1^2 + c_5\dot{\theta}_2^2 + c_6\dot{\theta}_3^2 + c_7\dot{\theta}_1\dot{\theta}_2 + c_8\dot{\theta}_2\dot{\theta}_3 + c_9\dot{\theta}_3\dot{\theta}_1 + c_{10}$$

Once this torque exceeds the friction torque, these equations will no longer be valid. Equations A.3.3, A.3.4, and A.3.5, then, decsribe the acceleration of the three generalized co-ordinates. However, once the torque on joint 3 exceeds the friction torque at joint 3, the program is stopped according to constraint 4 explained in chapter 5.1.

A.5 Linear velocity of center of mass

The linear velocity of center mass is a very important factor in analysing our model. The approach used to find the linear velocity of the three link model is presented in the following section. The approach for the two link model is similar and thus, not explained. Some of the notation used in this analysis is described below.

${}^{N}\omega^{A}$ = Angular velocity of frame A in frame B

${}^{N}V^{P}$ = Velocity of any point P in reference frame N

$\mathbf{n}_1$, $\mathbf{n}_2$, $\mathbf{n}_3$ are three mutually perpendicular vectors in a reference frame N

S_i and C_i represent $\sin\theta_i$ and $\cos\theta_i$ respectively

Kane's (1987) approach is used for developing expression for the linear velocity of center of mass. Each link in the model is considered to be a different frame, for ease of analysis. Frames A, B and C represent links 1, 2 and 3 respectively. N is the Newtonian reference frame. The three generalized coordinates are θ_1, θ_2 and θ_3. The three generalized speeds u_1, u_2 and u_3 represent $\dot{\theta}_1, \dot{\theta}_2$ and $\dot{\theta}_3$ respectively. Figure A.5.1 describes various reference frames. The bold letters **a**'s represent mutually perpendicular unit vectors in reference frame **A**. Similarly **b**'s and **c**'s represent mutually

perpendicular unit vectors in reference frames **B** and **C** respectively.

The angular velocities of the different frames and velocities of different points are given by,

$$^{N}\omega^{A} = \dot{\theta}_1 \mathbf{a}_3 = u_1 \mathbf{a}_3$$

$$^{N}\omega^{B} = \dot{\theta}_2 \mathbf{b}_3 = u_2 \mathbf{b}_3$$

$$^{N}\omega^{C} = \dot{\theta}_3 \mathbf{c}_3 = u_3 \mathbf{c}_3$$

$$^{N}\omega^{B} = {}^{N}\omega^{A} + {}^{A}\omega^{B} = u_1 \mathbf{a}_3 + u_2 \mathbf{b}_3$$

$$^{N}\omega^{C} = {}^{N}\omega^{A} + {}^{A}\omega^{B} + {}^{B}\omega^{C} = u_1 \mathbf{a}_3 + u_2 \mathbf{b}_3 + u_3 \mathbf{c}_3$$

$$^{N}V^{P1} = u_1 l_1 \mathbf{a}_2 \qquad \text{(A.5.1)}$$

$$^{N}V^{P2} = {}^{N}V^{P1} + {}^{N}\omega^{B} \times l_2 \mathbf{b}_1 = u_1 l_1 \mathbf{a}_2 + l_2 (u_1 + u_2) \mathbf{b}_2 \qquad \text{(A.5.2)}$$

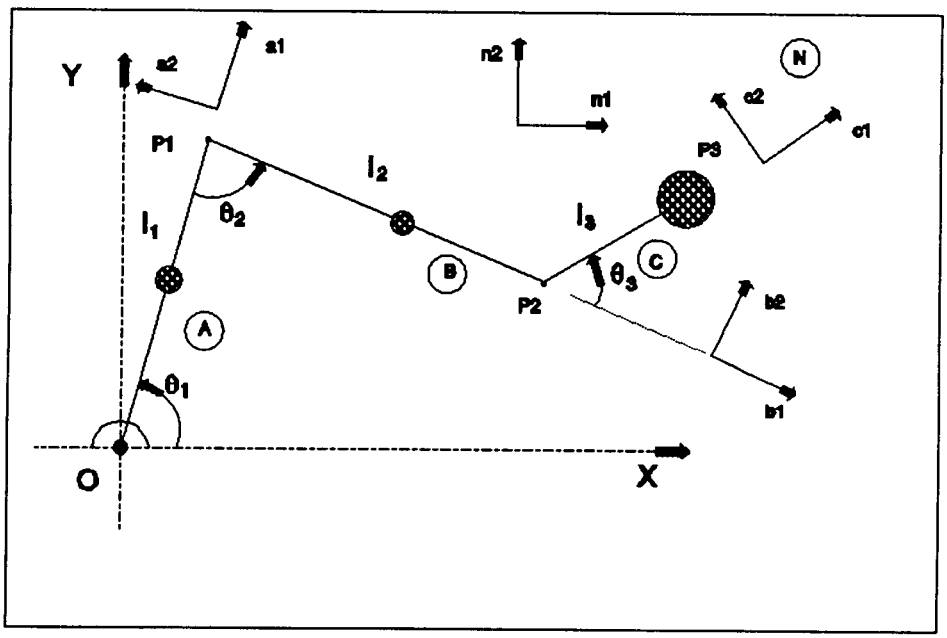

Fig A.5.1 Orientation of different frames

$$^{N}V^{P3} = {}^{N}V^{P2} + {}^{N}\omega^{C} \times l_3\mathbf{c}_1 = u_1 l_1 \mathbf{a}_2 + l_2(u_1+u_2)\mathbf{b}_2 + l_3(u_1+u_2+u_3)\mathbf{c}_2 \quad (A.5.3)$$

The relationship between different vectors in different reference frames can be represented as shown below.

$$\mathbf{a}_1 = C_1\mathbf{n}_1 + S_1\mathbf{n}_2$$

$$\mathbf{a}_2 = -S_1\mathbf{n}_1 + C_1\mathbf{n}_2$$

$$\mathbf{b}_1 = (S_1S_2-C_1C_2)\mathbf{n}_1 - (S_1C_2+C_1S_2)\mathbf{n}_2$$

$$\mathbf{b}_2 = (S_1C_2-S_2C_1)\mathbf{n}_1 + (S_1S_2-C_1C_2)\mathbf{n}_2$$

$$\mathbf{c}_1 = (C_3(S_1S_2-C_1C_2)+S_3(S_1C_2+C_1S_2))\mathbf{n}_1 - (C_3(S_1C_2+C_1S_2)$$
$$S_3(S_1S_2-C_1C_2))\mathbf{n}_2$$

$$\mathbf{c}_2 = (-S_3(S_1S_2-C_1C_2)+C_3(S_1C_2+C_1S_2))\mathbf{n}_1 - (S_3(S_1C_2+C_1S_2)$$
$$C_3(S_1S_2-C_1C_2))\mathbf{n}_2$$

Velocity of point P_3 in N can be written in terms of vectors n_1 and n_2 using equations A.5.1, A.5.2 and A.5.3. Simplifying the terms would result in an expression

$$^{N}V^{P3} = v_1\mathbf{n}_1 + v_2\mathbf{n}_2$$

where,

$$v_1 = -u_1l_1S_1 + l_2(u_1+u_2)(S_1C_2+C_1S_2) + l_3(u_1+u_2+u_3)(C_1C_2S_3-$$
$$S_1S_2S_3+S_1C_2C_3+C_1S_2C_3)$$

$$v_2 = -u_1l_1C_1 + l_2(u_1+u_2)(S_1S_2-C_1C_2) + l_3(u_1+u_2+u_3)(S_1C_2S_3+$$
$$C_1S_2S_3+S_1S_2C_3-C_1C_2C_3)$$

The magnitude and the direction w.r.t. ground of the linear velocity of center of mass is given by

$$v_{mag} = (v_1^2+v_2^2)^{1/2}$$

$$v_{direction} = \tan^{-1}(v_2/v_1)$$

APPENDIX B

FLOW CHARTS FOR SOFTWARE

The software consists of three main modules. The first module is the driver routine which calls the appropriate functions, i.e., for two-link or three-link model, and at the end of the program it calls the graphic routine for presentation on the screen. The second module is the differential equations module. This consists of two functions, one for each of the two models. The third module is the Runge-Kutta numerical integration routine. The driver routine calls this function to integrate the appropriate differential equations.

This appendix consists of the flow charts for the driver routine and the Runge-Kutta numerical integration routine. The other module, i.e., the differential equations module, is clearly explained in chapters 4 and 5. Figure B.1 illustrates the driver routine. Figure B.2 gives the flow chart for Runge-Kutta numerical integrations procedure.

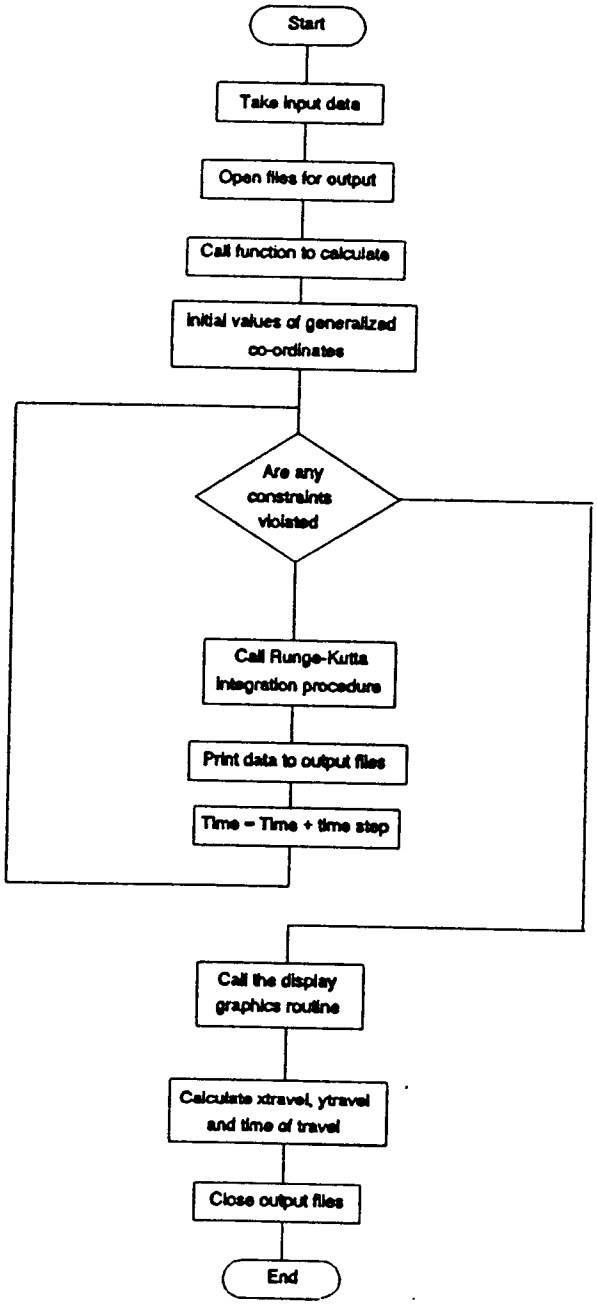

Fig B.1 Flow chart for driver routine for the software

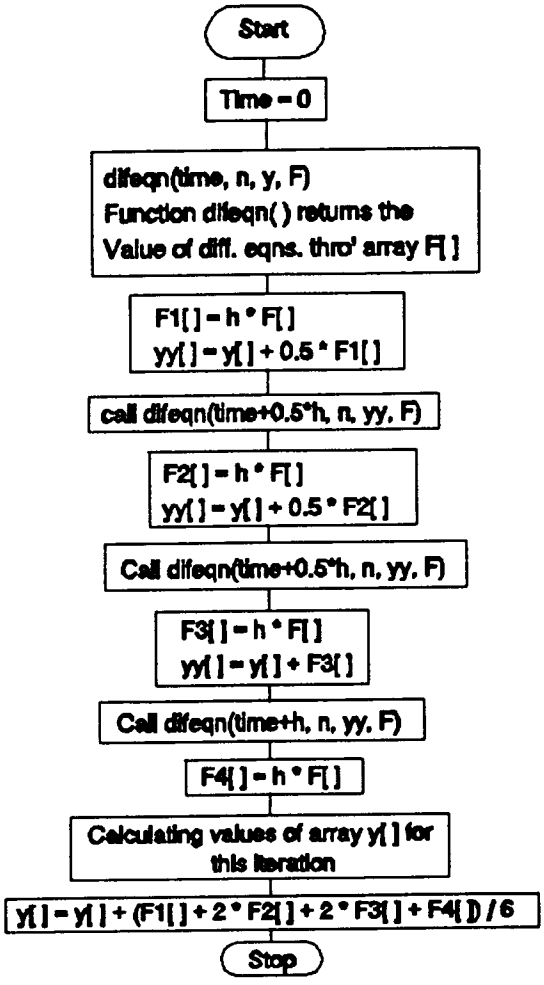

h = Time step

F[ ] = Array of values of first order differential eqns. evaluated at that particular time

y[ ] = Integrated values of the diff. eqns. after the previous iteration

n = array size (no. of diff. eqns.)

Fig B.2 Flow chart for Runge-Kutta numerical integration procedure